CAPITAL UNIVERSITY OF SCIENCE AND TECHNOLOGY, ISLAMABAD

Numerical Study of Viscous Dissipation and Cattaeno-Christov Heat Flux

by

Bilal Ali

A thesis submitted in partial fulfillment for the degree of Master of Philosophy

in the

Faculty of Computing
Department of Mathematics

2021

I dedicate this work to my beloved parents particularly my mother(late), who has been source of inspiration and gave me strength, who continuously provide her moral, spiritual and financial support.

To my all family members and my mentor my supervisor Dr. Muhammad sagheer who always guides me toward betterment in life.

CERTIFICATE OF APPROVAL

Numerical Study of Viscous Dissipation and Cattaneo-Christov Heat Flux

by

Bilal Ali

(MMT191024)

THESIS EXAMINING COMMITTEE

S. No.	Examiner	Name	Organization
(a)	External Examiner	Dr. Ahmed Zeeshan	IIUI, Islamabad
(b)	Internal Examiner	Dr. Rashid Ali	CUST, Islamabad
(c)	Supervisor	Dr. Muhammad Sagheer	CUST, Islamabad

Dr. Muhammad Sagheer
Thesis Supervisor
December, 2021

Dr. Muhammad Sagheer
Head
Dept. of Mathematics
December, 2021

Dr. Muhammad Abdul Qadir
Dean
Faculty of Computing
December, 2021

Author's Declaration

I, **Bilal ali** hereby state that my MPhil thesis titled "**Numerical Study of Viscous Dissipation and Cattaeno-Christov Heat Flux**" is my own work and has not been submitted previously by me for taking any degree from Capital University of Science and Technology, Islamabad or anywhere else in the country/abroad.

At any time if my statement is found to be incorrect even after my graduation, the University has the right to withdraw my MPhil Degree.

(Bilal Ali)

Registration No: MMT191024

Plagiarism Undertaking

I solemnly declare that research work presented in this thesis titled "**Numerical Study of Viscous Dissipation and Cattaeno-Christov Heat Flux**" is solely my research work with no significant contribution from any other person. Small contribution/help wherever taken has been duly acknowledged and that complete thesis has been written by me.

I understand the zero tolerance policy of the HEC and Capital University of Science and Technology towards plagiarism. Therefore, I as an author of the above titled thesis declare that no portion of my thesis has been plagiarized and any material used as reference is properly referred/cited.

I undertake that if I am found guilty of any formal plagiarism in the above titled thesis even after award of MPhil Degree, the University reserves the right to withdraw/revoke my MPhil degree and that HEC and the University have the right to publish my name on the HEC/University website on which names of students are placed who submitted plagiarized work.

(Bilal Ali)
Registration No: MMT191024

Acknowledgement

I got no words to articulate my cordial sense of gratitude to **Almighty Allah** who is the most merciful and most beneficent to his creation.

I also express my gratitude to the last prophet of **Almighty Allah, Prophet Muhammad (PBUH)** the supreme reformer of the world and knowledge for human being.

I would like to be thankful to all those who provided support and encouraged me during this work.

I would like to be grateful to my thesis supervisor **Dr. Muhammad Sagheer**, the Head of the Department of Mathematics, for guiding and encouraging towards writing this thesis. It would have remained incomplete without his endeavour. His profound expertise in the research field have been both asset and a source of inspiration. Also special thanks to **Dr. Shafqat Hussain** for his valuable suggestions and co-operation and all other faculty members.

A bundle of thanks are also for my parents who always prayed and financially assisted me for my achievements.

Bilal Ali

Abstract

In this thesis, the numerical investigation of the inertial and micro structure characteristics for magnetite ferrofluid flow over a linear stretching and shrinking sheet of the Cattaneo-Christov heat flux model with viscous dissipation has been considered. The governing non linear PDEs, are transformed into a system of dimensionless ODEs, by using similarity transformation. The reduced equation are then solved numerically with the aid of shooting method. The impact of different parameters such as nano particle volume fraction, micro rotation parameter, magnetic parameter, nonlinear stretching and shrinking parameter, Eckert number and chemical reaction parameter on the velocity profile, temperature distribution, skin friction and Nusselt number has been analyzed. The results obtained are shown in the form of table and graph. It is observed that the increase in the value of nanoparticle volume fraction, micro rotation parameter, and magnetic parameter the value of Nusselt number decreases. The results obtained reveal that there is an enhancement in the rate of heat transfer with a rise in the shrinking and the rate of heat transfer decreases by increasing the stretching of the sheet. The increasing values of Eckert number and chemical reaction parameter reduces the amount of heat transfer. The temperature distribution is also influenced by the presence of time relaxation parameter γ, thermal radiation R and nanoparticle volume fraction ϕ. This shows that the volume fraction of nanoparticles can be used in controlling the behavior of heat transfer and ferrofluid flows.

Contents

List of Figures

List of Tables

Abbreviations

IVPs	Initial values problems
ODEs	Ordineary differential equations
PDEs	Partial differential equations
RK	Runge-Kutta

Symbols

B_0	Magnetic field intensity
$(C_p)_{nf}$	Ferrofluid heat capacity
F	Dimensionless stream function
G	Dimensionless micro-rotation velocity
g	Acceleration due to gravity
I	Body coupled per unit mass
j	Micro inertia density
K	Micro-rotation parameter
κ	Mean absorption coefficient
κ_f	Base fluid thermal conductivity
κ_s	Ferroparticles thermal conductivity
κ_{nf}	Ferrofluid thermal conduvtivity
M	Magnetic parameter
$\boldsymbol{N}$	Micro-rotation vector
P	Pressure
Pr	Prandtl number
q_r	Radiative heat flux
S	Suction/injection parameter
T	Temperature of the fluid
T_w	Wall temperature
T_∞	Ambient temperature
u	x-component of velocity
v	y-component of velocity

$\boldsymbol{V}$	Velocity vector
Greek letter	
α	Stretching/shrinking parameter
λ	Spin gradient viscosity coefficient
ϕ	Nanoparticles volume fraction
κ	Vortex viscosity
μ_f	Base fluid dynamic viscosity
μ_{nf}	Ferrofluid dynamic viscosity
ρ_f	Base fluid density
ρ_s	Ferroparticles density
γ_{nf}	Spin gradient viscosity
δ	Boundary parameter
σ_f	Base fluid electrical conductivity
σ_s	Ferroparticle electrical conductivity
σ_{nf}	Ferrofluid electrical conductivity
σ^*	Stefan boltzman constant
θ	Dimensionless parameter
Subscripts	
f	Base fluid
s	Ferro particle
nf	Ferrofluid
w	Condition at wall
∞	Condition at infinity

Chapter 1

Introduction

The rate of flow of heat transfer is dependant on the thermal conductivity of working fluid, like water, oil and ethyl glycol. By adding a little portion of nanoparticles (like Cu, Ag, TiO_2 and Al_2O_3) into a traditional liquid, another class of liquids is acquired which is called nanofluids. Nanofluids cleared another pathway to developments in the improvement of the attributes of heat transfer. The nanotechnology is firstly used by Choi and Eastman [1]. After that, this research topic have been attracted the notice of several researcher of the world in perspective of its interesting heat transfer and potential application in several disciplines. After that many researchers participated in this field. Nanofluid has various application as nanofibres, nanowires, nanotubes and nanosheets [2]. Nanofluids pulled in the consideration of analysts because of immense uses of these liquids in car radiators, cooling of heat exchanging equipments, transformer oil cooling and electronic cooling [3, 4]. The diameter of the suspended nanoparticle varies between 1 to 100 nm. There seems a boost in the thermophysical properties of the ordinary liquid when the nanoparticle are suspended in it.

Pak and Cho [5] carry out an experiment on the turbulant transfer of heat flow of two kinds of drape nanoparticles γ-alumina (Al_2O_3) and titanium dioxide (TiO_2) nanofluid. The experimental study shows that the addition of nanoparticles increases the rate of transfer of heat in water. Eastman et al. [6] performed prior hypothesis with Cu water drape nano particles and observed that heat transfer coefficient is greater than that of observed for water in a refined state. Qiang and

Yimin [7] also observed that the addition of Cu in water produces much better than that of produced by Eastman [6]. Some more experiments are performed from Rashidi and Nezimabad [8], and Mahanta and Abramson [9], Sun et al. [10] and Walvekar et al. [11].

To review the practices of nanofluids, we mainly used two different models named as Buongiorno model [12] and Tiwari-Das model [13]. The Buongiorno model is mainly consist of few main mechanisms of slip between solid phases and fluid such as thermophoresis, fluid drainage, inertia, Brownian diffusion, magnus effect, diffusionphoresis and gravity settling while the Tiwari-Das model [13] is one of the example of single phase model. In single phase model the fluid, velocity and temperature they are taken as the same. There are few important influential mechanisms in the field of nanofluids such as Brownian diffusion and thermophoresis. Buongiorno model is used in many reserch articles by Buongiorno [12] and many others Kuznetsov et al. [14], Noghrehabadi et al. [15], Mutuku and Makinde [16], Xua and Pop [17], Khan and Makinde [18]. After that, this model has also been used to solve different numerical problems of nanofluids under stretching and shrinking case. For example, Zaimi et al. [19] observed heat transfer in nanofluid over a stretched and shrinked surface. Khan et al. [20] uses finite difference scheme for a convectively-heated stretching sheet by using third grade nano fluid model inside the presence of partial slip. Qasim et al. [21] considerd a thin film over a stretching sheet under the influence of magnetic field and observed the mass transfer of heat in nanofluid [21] analyzed the mass transfer of a heat in nanofluid. Akbar et al. [22] used numerical techniques for magneto-nanofluid over a stretched sheet by using Buongiorno model. Mohyud-Din et al. [23] calculated the flow of heat transfer and mass through different channels in nanofluids. Khan et al. [24] investigated the MHD flow of nano fluid over a non linear stretching and shrinking thrust. Recently, Sheikholeslami and Rokni [25] observed the effect of radiations on the heat transfer over a stretched sheet. Furthermore, many new developments on Buongiorno model are presented by Sheikholeslami et al. [26], Sheremet and Pop [27], Ahrar and Djavareshkian [28], Mustafa [29] and Ahmad et al. [30].

The next model is the Tiwari-Das model [13] which basically scrutinize the nano particles volume fraction in the base fluid inspite of the Brownian motion and

studied the rate of flow of heat and observed different charactrastics of naofluids under different physical situations. Later, this reserch topic has gained the attention of many reserchers to study the heat transfer charactrastics. Yu et al. [31] calculated the heat transfer of nanofluids which contain graphene oxide as a nanofluid and established that the increase in heat transfer is observed as compared to the ethylene glycol. Yacob et al. [32] considered the heat flow in Ag and Cu-water nanofluid over a shrinking and stretching surface. Vajravelu et al. [33] also observed the Cu-water and Ag-water nanoparticles, and observed free convection flow with internal heat absorption generation or over a stretching sheet. Other exemplary analysis on Tiwari-Das model are studied under variable conditions by using some different types of nanoparticles can be found in Hamad [34], Hamad et al. [35], Sheikholeslami et al. [36], Sheikholeslami and Ganji [37] and produced some great achievments. Alternatively, Ebaid and Sharif [38] consider magnetic field on CNTs nanofluids and observed flow of heat. The impact of chemical reaction with SWCNTs nanofluids and water based Cu, Al_20_3 is observed by Kandasamy et al. [39]. MHD water flow based on nanofluids containing Al_2O_3, Cu and TiO_2 over an accelerated plate was considerd by Abid Hussanan et al. [40]. Ebaid and sharif [38] work is extended by Saleh et al. [41] by considering both cases of injection and suction under the effect of convective condition. Both of these problems were solved through the utility of Laplace transformation.

The Micropolar theory was invented by Eringen [42]. It offers with the fluids which have some unique microscopic characters arise from the microrotation and neighborhood structure of the fluid elements. These fluids contain dilute suspensions of rigid macromolecules with individual motions that aid strain and body moments and are affected from spin inertia. The microrotation vector and gyration parameter are involve in such flow equations including the velocity vector. Hassanien and Gorla [43] talk about the heat transfer in streching surface. This issue was further expanded by Mohammadien and Gorla [44] added viscous and heat generation effects. Turkyilmazoglu [45] observed flow due to porous streching surface. Later on, newtonion heating was applied on micropoloar fluid by Hussanan et al. [46]. Some research articles are also available, for example Hussanan et al. [47],

Waqas et al. [48] and Saleh et al. [49], who studied micropolar model in the

presence of different conditions. When the nanoparticles are added in these type of nanofluids, it makes the mixture more complicated as compared to the conventional nanofluids. The research provide a new path way for reserchers to explore nanofluid characteristics. Tiwari and Das [13] uses Buongiorno model approach to study the micropolar nanofluid flow in the presence of stretching sheet. This difficulty was further studied by Hsiao [50] to comprise the viscous dessipation and observed its effects on MHD transfer of heat flow in the absence of chemical reaction.

The present work proposes the suspension of micropolar fluid Fe_3O_4 nanoparticles is supended in micropolar fluid. A mathematical model for the micropolar fluid flow in the existence of thermal radiation over a shrinking and stretching sheet subjected to injection and suction is based on Tiwari Das nano fluid model [13].

1.1 Thesis Contributions

The present survey is focused on the numerical analysis of inertial and microstructure charactrastics of a ferrofluid over a linear stretching and shrinking sheet [13]. The reviewed work is extended by considering Cattaneo-Christov heat flux model and viscous dessipation. The irreversible process by means of which the work done by a fluid on adjacent layers due to the action of shear forces is transformed into heat is defined as viscous dissipation and Cattaneo-Christov heat flux model is used to describe the heat transfer in viscoelastic flow induced by an exponentially stretching sheet. The proposed nonlinear PDEs are converted into system of ODEs by applying similarity transformations. The reduced equation are then solved numerically with the aid of shooting method. The numerically obtained results are computed by using MATLAB. The impact of significant parameters on velocity distribution $F'(\eta)$, temperature distribution $\theta(\eta)$ and skin friction C_{fx} and Nusselt number Nu_x have been discussed in graphs and tables.

1.2 Layout of Thesis

A brief overview of the contents of the thesis is provided below.

Chapter 2 includes some basic definitions and terminologies, which are useful to

understand the concepts discussed later on.

Chapter 3 provides the proposed analytical study of inertial and microstrucrure charactrastics of a nanofluid in the existence of stretching and shrinking sheet. The numerical results of the governing flow equations are derived by the shooting method.

Chapter 4 extends the proposed model flow discussed in Chapter 3 by using the nanofluid.

Chapter 5 provides the concluding remarks of the thesis.

References used in the thesis are mentioned in **Biblography**.

Chapter 2

Preliminaries

Some definitions, basic laws and terminologies would be discussed in the current chapter, which would be used in next chapters.

2.1 Some Basic Terminologies

Definition 2.1.1 (Fluid)

"A fluid is a substance that deforms continuously under the application of a shear (tangential) stress no matter how small the shear stress may be." [51]

Definition 2.1.2 (Fluid Mechanics)

"Fluid mechanics is that branch of science which deals with the behavior of the fluid (liquids or gases) at rest as well as in motion."[52]

Definition 2.1.3 (Fluid Dynamics)

"The study of fluid if the pressure forces are also considered for the fluids in motion, that branch of science is called fluid dynamics." [52]

Definition 2.1.4 (Fluid Statics)

"The study of fluid at rest is called fluid statics."[52]

Definition 2.1.5 (Viscosity)

"Viscosity is defined as the property of a fluid which offers resistance to the movement of one layer of fluid over another adjacent layer of the fluid. Mathematically,

$$\mu = \frac{\tau}{\frac{\partial u}{\partial y}},$$

where μ is viscosity coefficient, τ is shear stress and $\frac{\partial u}{\partial y}$ represents the velocity gradient." [52]

Definition 2.1.6 (Kinematic Viscosity)

"It is defined as the ratio between the dynamic viscosity and density of fluid. It is denoted by symbol ν called **nu**. Mathematically,

$$\nu = \frac{\mu}{\rho}."[52]$$

Definition 2.1.7 (Thermal Conductivity)

"The Fourier heat conduction law states that the heat flow is proportional to the temperature gradient. The coefficient of proportionality is a material parameter known as the thermal conductivity which may be a function of a number of variables." [53]

Definition 2.1.8 (Thermal Diffusivity)

"The rate at which heat diffuses by conducting through a material depends on the thermal diffusivity and can be defined as:

$$\alpha = \frac{k}{\rho C_p},$$

where α is the thermal diffusivity, k is the thermal conductivity, ρ is the density and C_p is the specifc heat at constant pressure." [54]

2.2 Viscous Dissipation

"The effects of viscous dissipation on the temperature field and ultimately on the friction factor have been investigated using dimensional analysis and experimentally validated computer simulations. Three common working fluids, i.e., water, methanol and iso-propanol, in different conduit geometries were considered. It turns out that for microconduits, viscous dissipation is a strong function of the channel aspect ratio, Reynolds number, Eckert number, Prandtl number and conduit hydraulic diameter. Thus, ignoring viscous dissipation could affect accurate flow simulations and measurements in microconduits."[55]

2.3 Cattaneo-Christov Heat Flux Model

"We make use of the Cattaneo Christov heat flux model to develop the equation of energy and investigate the qualities of surface heat transfer. The governing flow and energy equations are modified into the ordinary differential equations by similarity method for reasonable change. The subsequent ordinary differential equations are illuminated numerically through shooting method in MATLAB. The impact of different flow parameters for example thermal relaxation parameter, suction parameter, stretching/shrinking parameter, free stream parameter, and nanoparticles volume fraction on the skin friction coefficient, local Nusselt number, and streamlines are contemplated and exposed through graphs. It turns out that the lower branch solution for the skin friction coefficient becomes singular in shrinking area, although the upper branch solution is smooth in both stretching and shrinking domain. For oblique stagnation-point flow the streamlines pattern are not symmetric, and reversed phenomenon are detected close to the shrinking

surface. Also, we observed that the free stream parameter changes the direction of the oncoming flow and controls the obliqueness of the flow. The existing work mostly includes heat and mass transfer as a mechanism for improving the heat transfer rate, which is the main objective of the authors." [56]

2.4 Types of Fluid

"The fluid is classified into the following types"

Definition 2.2.1 (Ideal Fluid)

"A fluid, which is incompressible and has no viscosity, is known as an ideal fluid. Ideal fluid is only an imaginary fluid as all the fluids, which exist, have some viscosity." [52]

Definition 2.2.2 (Real Fluid)

"A fluid, which possesses viscosity, is known as a real fluid. In actual practice, all the fluids are real fluids." [52]

Definition 2.2.3 (Newtonian Fluid)

"A real fluid, in which the shear stress is directly proportional to the rate of shear strain (or velocity gradient), is known as a Newtonian fluid." [52]

Definition 2.2.4 (Non-Newtonian Fluid)

"A real fluid in which the shear stress is not directly proportional to the rate of shear strain (or velocity gradient), is known as a non-Newtonian fluid.

$$\tau_{xy} \propto \left(\frac{du}{dy}\right)^m, \qquad m \neq 1$$
$$\tau_{xy} = \mu\left(\frac{du}{dy}\right)^m.$$

Some examples of non-Newtonian fluids are toothpaste, shampoo, and honey etc." [52]

Definition 2.2.5 (Ideal Plastic Fluid)

"A fluid, in which the shear stress is more than the yield value and shear stress is proportional to the shear strain(or velocity gradient), is known as ideal plastic fluid

The examples of ideal plastic fluids is Water suspension of clay and fly ash" [52]

Definition 2.2.12 (Magnetohydrodynamics)

"Magnetohydrodynamics(MHD) is concerned with the mutual interaction of fluid flow and magnetic fields. The fluids in question must be electrically conducting and non-magnetic, which limits us to liquid metals, hot ionized gases (plasmas) and strong electrolytes." [57]

2.5 Types of Flow

"The flow of fluid is classified as"

Definition 2.3.1 (Rotational Flow)

"Rotational flow is that type of flow in which the fluid particles while flowing along stream-lines, also rotate about their own axis." [52]

Definition 2.3.2 (Irrotational Flow)

"Irrotational flow is that type of flow in which the fluid particles while flowing along stream-lines, do not rotate about their own axis." [52]

Definition 2.3.3 (Laminar Flow)

"Laminar flow is defined as that type of flow in which the fluid particles move along well-defined paths or stream line and all the stream-lines are straight and parallel." [52]

Definition 2.3.4 (Turbulent Flow)

"Turbulent flow is that type of flow in which the fluid particles move in a zig-zag way. Due to the movement of fluid particles in a zig-zag way." [52]

Definition 2.3.5 (Compressible Flow)

"Compressible flow is that type of flow in which the density of the fluid changes from point to point or in other words the density (ρ) is not constant for the fluid. Mathematically,

$$\rho \neq k,$$

where k is constant." [52]

Definition 2.3.6 (Incompressible Flow)

"Incompressible flow is that type of flow in which the density is constant for the fluid. Liquids are generally incompressible while gases are compressible, Mathematically,

$$\rho = k,$$

where k is constant." [52]

Definition 2.3.7 (Steady Flow)

"If the flow characteristics such as depth of flow, velocity of flow, rate of flow at any point in open channel flow do not change with respect to time, the flow is said to be steady flow. Mathematically,

$$\frac{\partial Q}{\partial t} = 0,$$

where Q is any fluid property." [52]

Definition 2.3.8 (Unsteady Flow)

"If at any point in an open channel flow, the velocity of flow, depth of flow or rate of flow changes with respect to time, the flow is said to be unsteady. Mathematically,

$$\frac{\partial Q}{\partial t} \neq 0,$$

where Q is any fluid property." [52]

Definition 2.3.9 (Internal Flow)

"Flows completely bounded by solid surfaces are called internal or pipe or duct flows." [51]

Definition 2.3.10 (External Flow)

"Flows over bodies immersed in an unbounded fluid are termed external flows." [51]

2.6 Modes of Heat Transfer and Properties

Definition 2.4.1 (Heat Transfer)

"Heat transfer is a branch of engineering that deals with the transfer of thermal energy from one point to another within a medium or from one medium to another due to the occurrence of a temperature difference." [53]

Definition 2.4.2 (Conduction)

"The transfer of heat within a medium due to a diffusion process is called conduction." [53]

Definition 2.4.3 (Convection)

"Convection heat transfer is usually defined as energy transport affected by the motion of a fluid. The convection heat transfer between two dissimilar media is governed by Newtons law of cooling." [53]

Definition 2.4.4 (Radiation)

"Radiation is the energy transfer due to the release of photons or electromagnetic waves from a surface volume. Radiation doesnt require any medium to transfer heat. The energy produced by radiation is transformed by electromagnetic waves." [53]

Definition 2.4.9 (Thermal Radiation)

"Thermal radiation is defined as radiant (electromagnetic) energy emitted by a medium and is solely due to the temperature of the medium." [53]

2.7 Dimensionless Numbers

Definition 2.5.1 (Eckert Number)

"It is a dimensionless number used in continuum mechanics. It describes the

relation between flows and the boundary layer enthalpy difference and it is used for characterized heat dissipation. Mathematically,

$$Ec = \frac{u^2}{C_p \nabla T}$$

where C_p denotes the specific heat." [53]

Definition 2.5.2 (Prandtl Number)

"It is the ratio between the momentum diffusivity ν and thermal diffusivity α. Mathematically, it can be defined as

$$Pr = \frac{\nu}{\alpha} = \frac{\frac{\mu}{\rho}}{\frac{k}{C_p \rho}} = \frac{\mu C_p}{k}$$

where μ represents the dynamic viscosity, Cp denotes the specific heat and k stands for thermal conductivity. The relative thickness of thermal and momentum boundary layer is controlled by Prandtl number. For small Pr, heat distributed rapidly corresponds to the momentum." [53]

Definition 2.5.3 (Nusselt Number)

"The hot surface is cooled by a cold fluid stream. The heat from the hot surface, which is maintained at a constant temperature, is diffused through a boundary layer and convected away by the cold stream. Mathematically,

$$Nu_x = \frac{qL}{k}$$

where q stands for the convection heat transfer, L for the characteristic length and k stands for thermal conductivity." [58]

Definition 2.5.4 (Skin Friction Coefficient)

"The steady flow of an incompressible gas or liquid in a long pipe of internal D. The mean velocity is denoted by u_w. The skin friction coefficient can be defined as

$$C_{fx} = \frac{2\tau_0}{\rho u_w^2}$$

where τ_0 denotes the wall shear stress and ρ is the density." [59]

Definition 2.5.6 (Reynolds Number)

"It is defined as the ratio of inertia force of a flowing fluid and the viscous force of the fluid. Mathematically,

$$Re_x = \frac{VL}{\nu},$$

where U denotes the free stream velocity, L is the characteristic length and ν stands for kinematic viscosity." [52]

2.8 Governing Laws

Definition 2.6.1 (Law of Conservation of Momentum)

"The principle of conservation of linear momentum (or Newtons Second Law of motion) states that the time rate of change of linear momentum of a given set of particles is equal to the vector sum of all the external forces acting on the particles of the set, provided newtons third law of action and reaction governs the internal forces. newtons second law can be written as

$$\frac{\partial \rho}{\partial t}\mathbf{v} + \nabla.[(\rho \mathbf{v}) \otimes \mathbf{v}] = \nabla.\rho + \rho \mathbf{f}$$

where $\otimes$ is the tensor (or dyadic) product of two vectors, ρ is the Cauchy stress tensor (N/m^2) and f is the body force vector, measured per unit mass and normally taken to be the gravity vector." [53]

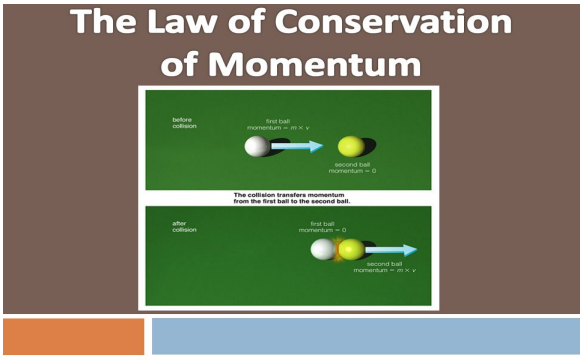

Definition 2.6.3 (Law of Conservation of Energy)

"The law of conservation of energy (or the First Law of Thermodynamics) states

that the time rate of change of the total energy is equal to the sum of the rate of work done by applied forces and the change of heat content per unit time. In the general case, the first law of thermodynamics can be expressed in conservation form as.

$$\frac{\partial \rho e^t}{\partial t} + \nabla.\rho \mathbf{v} e^t = -\nabla.\mathbf{q} + \nabla.(\sigma.\mathbf{v}) + Q + \rho \mathbf{f}.\mathbf{v}$$

where e^t = e + 1/2v v is the total energy (J/m^3), e is the internal energy, q is the heat flux vector (W/m^2) and Q is the internal heat generation (W/m^3)." [53]

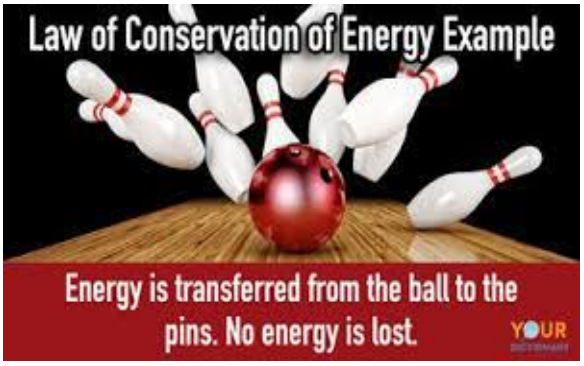

Definition 2.6.3 (Continuity Equation)

"The principle of conservation of mass can be stated as the time rate of change of mass in a fixed volume is equal to the net rate of flow of mass across the surface. The mathematical statement of the principle results in the following equation, known as the continuity (of mass) equation

$$\frac{\partial \rho}{\partial t} + \nabla.(\rho \mathbf{u}) = 0.$$

where ρ is the density (kg/m^3) of the medium, $\mathbf{v}$ the velocity vector (m/s), and ∇ is the nabla or del operator." [53]

2.9 Shooting Method

To elaborate the shooting method, consider the following nonlinear boundary value problem.

$$\left.\begin{aligned} &2y'''(x) + y(x)y''(x) = 0. \\ &y(0) = 0, \quad y'(0) = 0, \quad y'(g) = 1. \end{aligned}\right\} \tag{2.1}$$

To reduce the order of the above boundary value problem, introduce the following notations.

$$y = f_1 \qquad y' = f_1' = f_2 \qquad y'' = f_2' = f_3 \qquad y''' = f_3'. \tag{2.2}$$

As a result, (2.1) converted into the system of first order ODEs.

$$f_1' = f_2, \qquad f_1(0) = 0, \tag{2.3}$$

$$f_2' = f_3, \qquad f_2(0) = 0, \tag{2.4}$$

$$f_3' = -\frac{1}{2} f_1 f_3, \qquad f_3(0) = l, \tag{2.5}$$

where l is the missing initial condition which will be guessed.
The above IVP will be numerically solved by the RK-4 method. The missing condition l is to be chosen such that.

$$f_2(g, l) = 1. \tag{2.6}$$

For convenience, now onward, $f_2(g, l)$ will be denoted by $f_2(l)$.
Let us further denote $f_2(l) - 1$ by $H(l)$, so that

$$H(l) = 0. \tag{2.7}$$

The above equation can be solved by using Newton's method, which has the following iterative formula.

$$l^{n+1} = l^n - \frac{H(l^n)}{\frac{\partial H(l^n)}{\partial l}},$$

$$l^{n+1} = l^n - \frac{f_2(l^n) - 1}{\frac{\partial f_2(l^n)}{\partial l}}. \tag{2.8}$$

To find $\frac{\partial f_2(l^n)}{\partial l}$, introduce the following notations.

$$\frac{\partial f_1}{\partial l} = f_4, \quad \frac{\partial f_2}{\partial l} = f_5, \quad \frac{\partial f_3}{\partial l} = f_6. \tag{2.9}$$

As a result of these new notations, the Newton's iterative scheme, will then get the following form.

$$l^{n+1} = l^n - \frac{f_2(l) - 1}{f_5(l)}. \tag{2.10}$$

Now differentiating the system of two first order ODEs (2.3)-(2.5) with respect to l, we get another system of ODEs, as follows.

$$f_4' = f_5, \qquad f_4(0) = 0. \tag{2.11}$$

$$f_5' = f_6, \qquad f_5(0) = 0. \tag{2.12}$$

$$f_6' = -\frac{1}{2}\left[f_1 f_6 + f_3 f_4\right], \qquad f_6(0) = 1. \tag{2.13}$$

Writing all the six ODEs (2.3), (2.4), (2.5), (2.11), (2.12) and (2.13) together, we have the following initial value problem.

$$\begin{aligned}
f_1' &= f_2, & f_1(0) &= 0.\\
f_2' &= f_3, & f_2(0) &= 0.\\
f_3' &= -\frac{1}{2} f_1 f_3, & f_3(0) &= l.\\
f_4' &= f_5, & f_4(0) &= 0.\\
f_5' &= f_6, & f_5(0) &= 0.\\
f_6' &= -\frac{1}{2}\left[f_1 f_6 + f_3 f_4\right], & f_6(0) &= 1.
\end{aligned}$$

The above system together will be solved numerically by Runge-Kutta method of order four. The missing condition will be updated by the Newton's formula in (2.10).

The stopping criteria for the Newton's technique is set as,

$$\mid f_2(l) - 1 \mid < \epsilon,$$

where $\epsilon > 0$ is an arbitrarily small positive number.[60]

Chapter 3

Inertial and Micro structure Characteristics for Magnetite Ferrofluid using Tiwari and Das Model

3.1 Introduction

The numerical analysis of a ferrofluid flow towards a stretching and shrinking sheet using Tiwari and Das [13] conductivity model has been performed in this chapter. The governing non linear PDEs, are transformed into a system of dimensionless ODEs, by using similarity transformation. The reduced equation are then solved numerically with the aid of shooting method. At the end of this chapter, numerical solutions for several parameters are discussed for the dimensionless velocity and temperature distributions. The numerical results are expressed through tables and graphs. This chapter contains a detailed review of micro structure and inertial characteristic of a ferrofluid over a stretching and shrinking sheet by using effective thermal conductivity model [47].

3.2 Mathematical Modeling

A steady two-dimensional boundary layer flow of a micropolar ferrofluid over a stretching and shrinking sheet has been considered. These fluids deals with certain microscopic characters arising from the local structure and microrotation of the fluid elements. The flow equations of such fluids involve micro-rotation vector and gyration parameter in addition to the velocity vector. For a stretching and shrinking case a magnetic field B_0 is applied perpendicular to the sheet and the velocity is assumed as $u_w(x) = ax$. Under these assumptions, the flow of micropolar Ferrofluid is governed by the following equations (3.1)-(3.4). Furthermore by using shooting technique, the solution of ODEs are obtained. At the end of this chapter, the numerical outcomes against various parameters have been discussed.

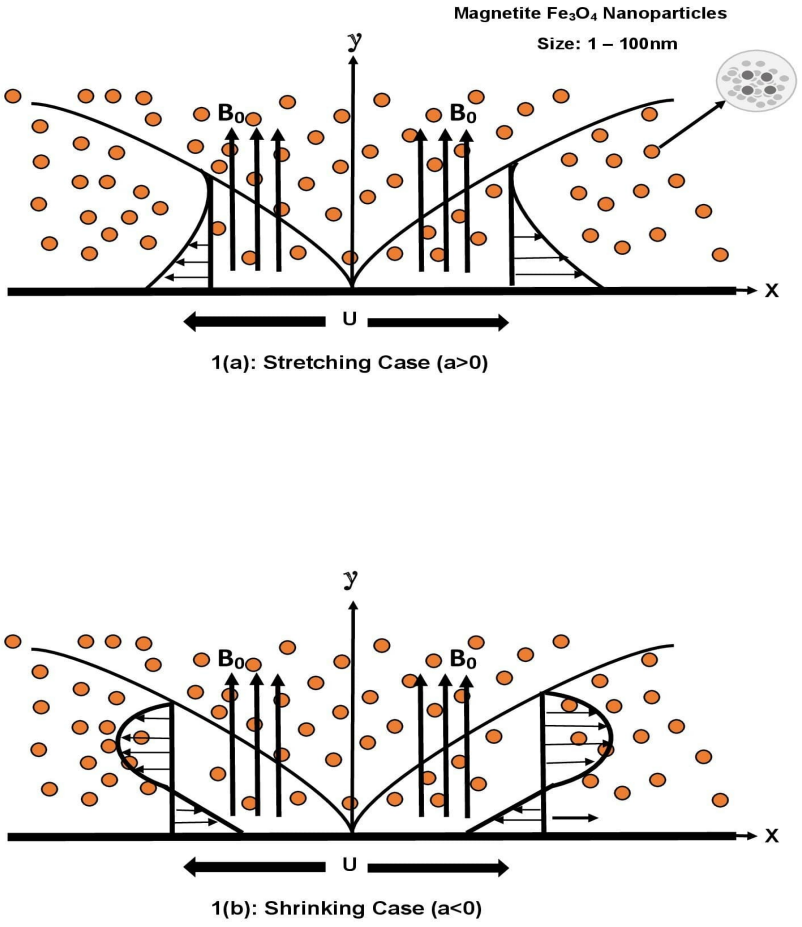

1. (a): Stretching Case (a>0). (b) Shrinking Case (a<0)

$$\frac{\partial u}{\partial x}+\frac{\partial v}{\partial y}=0, \tag{3.1}$$

$$\rho_{nf}\left(u\frac{\partial u}{\partial x}+v\frac{\partial u}{\partial y}\right)=(\mu_{nf}+k)\frac{\partial^2 u}{\partial y^2}+k\frac{\partial N}{\partial y}-\sigma_{nf}B_o^2 u, \tag{3.2}$$

$$\rho nfj\left(u\frac{\partial N}{\partial x}+v\frac{\partial N}{\partial y}\right)=\gamma_{nf}\frac{\partial^2 N}{\partial y^2}-k\left(2N+\frac{\partial u}{\partial x}\right), \tag{3.3}$$

$$u\frac{\partial T}{\partial x}+v\frac{\partial T}{\partial y}=\frac{k_{nf}}{(\rho c_p)_{nf}}\frac{\partial^2 T}{\partial^2 y}-\frac{\partial q_r}{\partial y}. \tag{3.4}$$

The associated boundary conditions are:

$$\begin{aligned}
&u=\alpha u_w(x), \quad v=v_w \quad at \quad y=0; \quad u\to 0 \quad as\ y\to\infty,\\
&N=-\delta\frac{\partial u}{\partial y} \qquad\qquad at \quad y=0; \quad N\to 0 \quad as \quad y\to\infty,\\
&T=T_w \qquad\qquad\qquad at \quad y=0; \quad T\to T_\infty \quad as \quad y\to\infty,
\end{aligned}$$

where v_w is the surface mass transfer velocity and corresponds to suction for $v_w>0$ and injection for $v_w<0$. The parameter δ is the micro gyration vector and the value of δ varies in the interval [0,1].

3.3 Conversion of PDEs to ODEs

To convert the partial differential equations into ordinary differential equations, we will use the following transformations.

$$\eta=y\sqrt{\frac{a}{v_f}},\ u=axF'(\eta),\ v=-\sqrt{av_f}F(\eta),\ N=ax\sqrt{\frac{a}{v_f}}G(\eta),$$
$$\theta(\eta)=\frac{T-T_\infty}{T_w-T_\infty}.$$

Here T_w and T_∞ are the temperatures at the wall and close to the other end of the boundary layer respectively.

Following are the derivatives used to convert the partial differential equations (3.1)-(3.4) into ordinary differential equations.

- $u=axF'(\eta)$,

$$\frac{\partial u}{\partial x} = aF'(\eta). \tag{3.5}$$

$$\frac{\partial u}{\partial y} = ax\sqrt{\frac{a}{v_f}}F''(\eta). \tag{3.6}$$

$$\frac{\partial^2 u}{\partial y^2} = \frac{a^2 x}{v_f}F''(\eta). \tag{3.7}$$

- $v = -\sqrt{av_f}F(\eta)$,

$$\frac{\partial v}{\partial x} = 0. \tag{3.8}$$

$$\frac{\partial v}{\partial y} = -aF'(\eta). \tag{3.9}$$

- $N = ax\sqrt{\frac{a}{v_f}}G(\eta)$,

$$\frac{\partial N}{\partial x} = a\sqrt{\frac{a}{\nu_f}}G(\eta). \tag{3.10}$$

$$\frac{\partial N}{\partial y} = \frac{a^2 x}{v_f}G'(\eta). \tag{3.11}$$

$$\frac{\partial^2 N}{\partial y^2} = \frac{a^{\frac{5}{2}}x}{v_f^{\frac{3}{2}}}G''(\eta). \tag{3.12}$$

- $T = \theta(\eta)(T_w - T_\infty) + T_\infty$,

$$\frac{\partial T}{\partial x} = 0. \tag{3.13}$$

$$\frac{\partial T}{\partial y} = (T_w - T_\infty)\sqrt{\frac{a}{\nu_f}}\theta'(\eta). \tag{3.14}$$

$$\frac{\partial^2 T}{\partial y^2} = (T_w - T_\infty)\frac{a}{\nu_f}\theta''(\eta). \tag{3.15}$$

Following are some useful formulae including those relating some physical properties of nanofluids to those of the base fluids.

$$\gamma_{nf} = \left(\mu_f + \frac{\kappa}{2}\right)j, \tag{3.16}$$

$$j = \frac{\nu_f}{a}, \tag{3.17}$$

$$\rho_{nf} = (1-\phi)\rho_f + \phi\rho_s, \tag{3.18}$$

$$\mu_{nf} = \frac{\mu_f}{(1-\phi)^{2.5}}, \tag{3.19}$$

$$\frac{\kappa_{nf}}{\kappa_f} = \frac{\kappa_s + 2\kappa f - 2\phi(\kappa_f - \kappa_s)}{\kappa_s + 2\kappa f + \phi(\kappa_f - \kappa_s)}, \tag{3.20}$$

$$(C_p)_{nf} = \frac{\phi(\rho C_p)_s + (1-\phi)(\rho C_p)_f}{\rho_{nf}}, \tag{3.21}$$

$$\sigma_{nf} = \left(1 + \frac{3(\sigma-1)\phi}{(\sigma+2)-(\sigma-1)\phi}\right)\sigma_f, \tag{3.22}$$

$$S = \frac{-v_w}{\sqrt{a\nu_f}}. \tag{3.23}$$

Furthermore, following notations will also be used in the conversion of the partial differential equations to the ordinary differential equations.

$$H_1 = \frac{1}{(1-\phi)^{5/2}}, \tag{3.24}$$

$$H_2 = H_1 + k, \tag{3.25}$$

$$H_3 = (1-\phi+\phi\frac{\rho_s}{\rho_f}), \tag{3.26}$$

$$H_4 = 1 + \frac{3(\sigma-1)\phi}{\sigma+2-(\sigma-1)\phi}, \tag{3.27}$$

$$H_5 = H_1 + \frac{k}{2} \tag{3.28}$$

$$H_6 = \frac{\left(\frac{\kappa_s+2\kappa_f-2\phi(\kappa_f-\kappa_s)}{\kappa_s+2\kappa_f+\phi(\kappa_f-\kappa_s)} + R\right)}{Pr}, \tag{3.29}$$

$$P_r = \frac{\nu_f\left(\rho C_P\right)_f}{\kappa_f}, \tag{3.30}$$

$$H_7 = 1-\phi+\phi\frac{(\rho C_p)_s}{(\rho C_p)_f}, \tag{3.31}$$

$$M = \frac{\sigma_f B_O^2}{\alpha\rho_f}. \tag{3.32}$$

$$\gamma = h_s\sqrt{\frac{\nu_f}{a}}, \tag{3.33}$$

$$K = \frac{\kappa}{\mu_f}, \tag{3.34}$$

$$R = \frac{16\sigma^* T_\infty}{3\kappa^*\kappa_f}. \tag{3.35}$$

3.3.1 Equation of Continuity

From (3.5) and (3.9) we have,

$$\frac{\partial u}{\partial x} = aF'(\eta),$$
$$\frac{\partial v}{\partial y} = -aF'(\eta).$$

Putting these two expressions in (3.1), we get

$$aF' - aF' = 0.$$

Hence the continuity equation is identically satisfied.

3.3.2 Momentum Equations

$$\rho_{nf}\left(u\frac{\partial u}{\partial x} + v\frac{\partial u}{\partial y}\right) = (\mu_{nf} + k)\frac{\partial^2 u}{\partial y^2} + k\frac{\partial N}{\partial y} - \sigma_{nf}B_o^2 u.$$

Using (3.5), (3.6), (3.7), (3.19) and (3.22) in (3.2), we get

$$\begin{aligned}
&((1-\phi)\rho_f + \phi\rho_s)\left(a^2xF'^2(\eta) - a^2xF(\eta)F''(\eta)\right) = \left(\frac{\mu_f}{1-\phi^{2.5}} + \kappa\right)\\
&\frac{a^2x}{v_f}F'''(\eta) + \kappa\left(\frac{a^2x}{v_f}G'(\eta)\right) - \left(1 - \frac{3(\sigma-1)\phi}{(\sigma+2)-(\sigma-1)\phi}\right)\frac{\sigma_f Ma\rho_f axF'(\eta)}{\sigma_f},\\
\Rightarrow &\left(1-\phi+\phi\frac{\rho_s}{\rho_f}\right)\left(F'^2(\eta) - F(\eta)F''(\eta)\right) = \frac{F'''(\eta)}{\nu_f\rho_f}\left(\frac{\mu_f}{(1-\phi)^{2.5}}\right) + \frac{\kappa G'(\eta)}{\nu_f\rho_f}\\
&- \left(1 - \frac{3(\sigma-1)\phi}{(\sigma+2)-(\sigma-1)\phi}\right)\frac{M\rho_f F'(\eta)}{\rho_f}.\\
\Rightarrow &\left(1-\phi+\phi\frac{\rho_s}{\rho_f}\right)F'^2(\eta) - \left(1-\phi+\phi\frac{\rho_s}{\rho_f}\right)F(\eta)F''(\eta)\\
&= \frac{\mu_f F'''(\eta)}{\rho_f\nu_f}\left(\frac{1}{1-\phi^{2.5}} + \frac{\kappa}{\mu_f}\right) + \frac{\kappa G'(\eta)}{\mu_f} - \left(1 - \frac{3(\sigma-1)\phi}{(\sigma+2)-(\sigma-1)}\right)MF'(\eta).\\
\Rightarrow &\left(\frac{1}{(1-\phi)^{2.5}} + \frac{\kappa}{\mu_f}\right)F'''(\eta) + \left(1-\phi+\phi\frac{\rho_s}{\rho_f}\right)F(\eta)F''(\eta)\\
&- \left(1-\phi+\phi\frac{\rho_s}{\rho_f}\right)F'^2(\eta) - \left(1 - \frac{3(\sigma-1)\phi}{(\sigma+2)-(\sigma-1)}\right)MF'(\eta) + kG'(\eta) = 0.
\end{aligned}$$

By using (3.25), (3.26) and (3.27), (3.32), (3.34) in the above equation,the following is achieved

$$H_2F'''(\eta) + H_3FF''(\eta) - H_3F'^2(\eta) - MH_4F'(\eta) + KG'(\eta) = 0. \tag{3.36}$$

Now the equation (3.3) will be converted to the dimensionless form through the following procedure.

Using (3.5), (3.10) and (3.11) and (3.12) in (3.3), we have

$$\rho_{nf} j \left(ua\sqrt{\frac{a}{\nu_f}} G(\eta) + v\frac{a^2 x G'(\eta)}{\nu_f} \right) = \gamma_{nf} \left(\frac{a^2 x G''(\eta)}{\nu_f} \sqrt{\frac{a}{\nu_f}} \right) - \kappa \left(2N + axF''(\eta) \sqrt{\frac{a}{\nu_f}} \right),$$

Using equation (3.17), we have

$$\rho_{nf} \frac{\nu_f}{a} \left(ua\sqrt{\frac{a}{\nu_f}} G(\eta) + v\frac{a^2 x G'(\eta)}{\nu_f} \right) = \gamma_{nf} \left(\frac{a^2 x G''(\eta)}{\nu_f} \sqrt{\frac{a}{\nu_f}} \right) - \kappa \left(2N + axF''(\eta) \sqrt{\frac{a}{\nu_f}} \right).$$

Using (3.16) and (3.18) in the above equation,we get

$$\begin{aligned}
&\left((1 - \phi\rho_f + \phi\rho_s) \frac{\nu_f}{a} \right) \left(ua\sqrt{\frac{a}{\nu_f}} G(\eta) + \frac{va^2 x G'(\eta)}{\nu_f} \right) = \left(\mu_{nf} + \frac{\kappa}{2} \right) \frac{\nu_f}{a} \\
&\left(\frac{a^2 x G''(\eta)}{\nu_f} \sqrt{\frac{a}{\nu_f}} \right) - \kappa \left(2N + axF''(\eta) \sqrt{\frac{a}{\nu_f}} \right). \\
\Rightarrow &\left((1 - \phi\rho_f + \phi\rho_s) \frac{\nu_f}{a} \right) \left(axF'(\eta) a\sqrt{\frac{a}{\nu_f}} G(\eta) - \frac{\sqrt{a}\nu_f a^2 x G'(\eta)}{\nu_f} \right) \\
&= \left(\mu_{nf} + \frac{\kappa}{2} \right) \frac{\nu_f}{a} \left(\frac{a^2 x G''(\eta)}{\nu_f} \sqrt{\frac{a}{\nu_f}} \right) - \kappa \left(2ax\sqrt{\frac{a}{\nu_f}} G(\eta) + axF''(\eta) \sqrt{\frac{a}{\nu_f}} \right). \\
\Rightarrow &\left((1 - \phi\rho_f + \phi\rho_s) \frac{\nu_f}{a} \right) \left(aF' \sqrt{\frac{a}{\nu_f}} G(\eta) - a\sqrt{\frac{a}{\nu_f}} F(\eta) G'(\eta) \right) \\
&= \left(\mu_{nf} + \frac{\kappa}{2} \right) \frac{\nu_f}{a} \left(\frac{a}{\nu_f} G''(\eta) \sqrt{\frac{a}{\nu_f}} \right) - \kappa \left(2\sqrt{\frac{a}{\nu_f}} G(\eta) + \sqrt{\frac{a}{\nu_f}} F''(\eta) \right). \\
\Rightarrow &((1 - \phi)\rho_f + \phi\rho_s) \nu_f \left(F'(\eta) G(\eta) - F(\eta) G'(\eta) \right) = \left(\mu_{nf} + \frac{\kappa}{2} \right) G''(\eta) \\
&- \kappa 2G(\eta) + F''(\eta). \\
\Rightarrow &(\rho_f \nu_f) \left(1 - \phi + \phi\frac{\rho_s}{\rho_f} \right) \left(F'(\eta) G(\eta) - FG'(\eta) \right) = \left(\frac{\mu_f}{1 - \phi^{2.5}} + \frac{\kappa}{2} \right) G''(\eta) \\
&- \kappa 2G(\eta) + F''(\eta), \\
\Rightarrow &\mu_f \left(1 - \phi + \phi\frac{\rho_s}{\rho_f} \right) \left(F'(\eta) G(\eta) - F(\eta) G'(\eta) \right) = \mu_f \left(\frac{1}{1 - \phi^{2.5}} + \frac{\kappa}{2\mu_f} \right) G''(\eta) \\
&- \kappa \left(2G(\eta) + F''(\eta) \right). \\
\Rightarrow &\left(1 - \phi + \phi\frac{\rho_s}{\rho_f} \right) \left(F'(\eta) G(\eta) - F(\eta) G'(\eta) \right) = \mu_f \left(\frac{1}{1 - \phi^{2.5}} + \frac{\kappa}{2\mu_f} \right) G''(\eta)
\end{aligned}$$

$$
\begin{aligned}
&- \frac{\kappa}{\mu_f}\left(2G(\eta) + F''(\eta)\right).\\
\Rightarrow &\left(\frac{1}{(1-\phi)^{2.5}} + \frac{\kappa}{2\mu_f}\right) G''(\eta) - \left(1 - \phi + \phi\frac{\rho_s}{\rho_f}\right) F'(\eta) + \left(1 - \phi + \phi\frac{\rho_s}{\rho_f}\right) F(\eta)G'(\eta)\\
&- \frac{\kappa}{\mu_f}\left(2G(\eta) + F''(\eta)\right) = 0.
\end{aligned}
$$

By using (3.24), (3.26) and (3.34), we get

$$
\begin{aligned}
&\left(H_1 + \frac{k}{2}\right) G''(\eta) + H_3 F(\eta)G'(\eta) - H_3 F'(\eta)G(\eta) - k(2G(\eta) + F''(\eta)) = 0.\\
\Rightarrow\ & H_5 G''(\eta) + H_3 F(\eta)G'(\eta) - H_3 F'(\eta)G(\eta) - k\left(2G(\eta) + F''(\eta)\right) = 0. \qquad (3.37)
\end{aligned}
$$

3.3.3 Energy Equation

Using (3.13), (3.14), (3.15) in (3.20), we have

$$
\begin{aligned}
&u(0) - v\theta'(\eta)\left(T_w - T_\infty\right)\sqrt{\frac{a}{\nu_f}} = \frac{\kappa_f}{(\rho C_p)_{nf}}\left[\frac{\kappa_s + 2\kappa_f - 2\phi(\kappa_f - \kappa_s)}{\kappa_s + 2\kappa_f + \phi(\kappa_f - \kappa_s)} + \frac{16\sigma^* T_\infty^3}{3\kappa^*\kappa_f}\right]\theta''(T_w - T_\infty)\frac{a}{\nu_f}.\\
\Rightarrow\ & axF'(\eta)(0) - \sqrt{a\nu_f}F'(\eta)\theta'(\eta)\left(T_w - T_\infty\right)\sqrt{\frac{a}{\nu_f}}\\
&= \frac{\kappa_f}{(\rho C_p)_{nf}}\left[\frac{\kappa_s + 2\kappa_f - 2\phi(\kappa_f - \kappa_s)}{\kappa_s + 2\kappa_f + \phi(\kappa_f - \kappa_s)} + \frac{16\sigma^* T_\infty^3}{3\kappa^*\kappa_f}\right]\theta''(\eta)(T_w - T_\infty)\frac{a}{\nu_f}.\\
\Rightarrow\ & axF'(\eta)(0) - \sqrt{a\nu_f}F'(\eta)\theta'(\eta)\sqrt{\frac{a}{\nu_f}}\\
&= \frac{\kappa_f}{(\rho C_p)_{nf}}\left[\frac{\kappa_s + 2\kappa_f - 2\phi(\kappa_f - \kappa_s)}{\kappa_s + 2\kappa_f + \phi(\kappa_f - \kappa_s)} + \frac{16\sigma^* T_\infty^3}{3\kappa^*\kappa_f}\right]\theta''(\eta)\frac{a}{\nu_f}.\\
\Rightarrow\ & -aF(\eta)\theta'(\eta) = \frac{\kappa_f}{(\rho C_p)_{nf}}\left[\frac{\kappa_s + 2\kappa_f - 2\phi(\kappa_f - \kappa_s)}{\kappa_s + 2\kappa_f + \phi(\kappa_f - \kappa_s)} + \frac{16\sigma^* T_\infty^3}{3\kappa^*\kappa_f}\right]\frac{\theta''(\eta)a}{\nu_f}.\\
\Rightarrow\ & \frac{-aF(\eta)\theta'(\eta)}{a} = \frac{\kappa_f}{(\rho C_p)_{nf}}\left[\frac{\kappa_s + 2\kappa_f - 2\phi(\kappa_f - \kappa_s)}{\kappa_s + 2\kappa_f + \phi(\kappa_f - \kappa_s)} + \frac{16\sigma^* T_\infty^3}{3\kappa^*\kappa_f}\right]\frac{\theta''(\eta)a}{a\nu_f}.\\
\Rightarrow\ & F(\eta)\theta'(\eta) = \frac{\kappa_f}{(\rho C_p)_{nf}}\left[\frac{\kappa_s + 2\kappa_f - 2\phi(\kappa_f - \kappa_s)}{\kappa_s + 2\kappa_f + \phi(\kappa_f - \kappa_s)} + \frac{16\sigma^* T_\infty^3}{3\kappa^*\kappa_f}\right]\frac{\theta''(\eta)}{\nu_f}.\\
\Rightarrow\ & F(\eta)\theta'(\eta) = \frac{\kappa_f}{\phi(\rho C_p)_s + (1-\phi)(\rho C_p)_f}\left[\frac{\kappa_s + 2\kappa_f - 2\phi(\kappa_f - \kappa_s)}{\kappa_s + 2\kappa_f + \phi(\kappa_f - \kappa_s)} + \frac{16\sigma^* T_\infty^3}{3\kappa^*\kappa_f}\right]\frac{\theta''(\eta)}{\nu_f}.
\end{aligned}
$$

$$\Rightarrow -\left((\rho C_p)_s + (1-\phi)(\rho C_p)_f\right) F(\eta)\theta'(\eta) = \kappa_f \left[\frac{\kappa_s + 2\kappa_f - 2\phi(\kappa_f - \kappa_s)}{\kappa_s + 2\kappa_f + \phi(\kappa_f - \kappa_s)} + R\right]\frac{\theta''(\eta)}{\nu_f}.$$

$$\Rightarrow -\left(\rho C_P\right)_f (1-\phi+\phi)\frac{\left(\rho C_P\right)_s}{\left(\rho C_P\right)_f} F(\eta)\theta'(\eta) = \kappa_f \left[\frac{\kappa_s + 2\kappa_f - 2\phi(\kappa_f - \kappa_s)}{\kappa_s + 2\kappa_f + \phi(\kappa_f - \kappa_s)} + R\right]\frac{\theta''(\eta)}{\nu_f}.$$

$$\Rightarrow -(1-\phi+\phi)\frac{\left(\rho C_P\right)_s}{\left(\rho C_P\right)_f} F(\eta)\theta'(\eta) = \frac{\kappa_f}{\left(\rho C_P\right)_f}\left[\frac{\kappa_s + 2\kappa_f - 2\phi(\kappa_f - \kappa_s)}{\kappa_s + 2\kappa_f + \phi(\kappa_f - \kappa_s)} + R\right]\frac{\theta''(\eta)}{\nu_f}.$$

Using (3.30) and (3.31) we get

$$-H_7 F(\eta)\theta'(\eta) = \left[\frac{\kappa_s + 2\kappa_f - 2\phi(\kappa_f - \kappa_s)}{\kappa_s + 2\kappa_f + \phi(\kappa_f - \kappa_s)} + R\right]\frac{\theta''(\eta)}{P_r}, \tag{3.38}$$

$$\Rightarrow H_6\theta''(\eta) + H_7 F(\eta)\theta'(\eta) = 0. \tag{3.39}$$

3.4 Conversion of Conditions

- $u = \alpha u_w(x)$ at $y = 0$,

$\Rightarrow (ax)F'(\eta) = \alpha(ax)$ at $\eta = 0$.

$\Rightarrow F'(0) = \alpha$.

- $v = v_w$ at $y = 0$,

$\Rightarrow -\sqrt{av_f}F(\eta) = -\sqrt{av_f}S$ at $\eta = 0$.

$\Rightarrow F(0) = S$.

- $N = -\delta\dfrac{\partial u}{\partial x}$ at $y = 0$,

$\Rightarrow -\delta\dfrac{\partial u}{\partial x} = ax\sqrt{\dfrac{a}{v_f}}G(0)$ at $\eta = 0$.

$\Rightarrow -\delta ax F''(0)\sqrt{\dfrac{a}{v_f}} = ax\sqrt{\dfrac{a}{v_f}}G(0)$.

$\Rightarrow G(0) = -\delta F''(0)$.

$$\Rightarrow G(0) = -\delta F''(0).$$

- $\theta(\eta) = \dfrac{T - T_\infty}{T_w - T_\infty}$ at $T = T_w$,

$\Rightarrow \theta(0) = \dfrac{T_w - T_\infty}{T_w - T_\infty}.$ at $\eta = 0$,

$$\Rightarrow \theta(0) = 1.$$

- $u \to 0,$ $as \;\; y \to 0.$

$$\Rightarrow axF'(\eta) \to 0,$$

$$\Rightarrow F'(\eta) \to 0, \qquad as \;\; \eta \to \infty,$$

$$\Rightarrow F'(\infty) \to 0.$$

- $G(\eta) \to 0.$ $as \;\; \eta \to \infty.$
- $T \to T_\infty,$ $as \;\; \eta \to \infty,$

$$\Rightarrow \theta(\eta)(T_w - T_\infty) + T_\infty \to T_\infty,$$

$$\Rightarrow \theta(\eta)(T_w - T_\infty) \to 0,$$

$$\Rightarrow \theta(\eta) \to 0, \qquad as \;\; \eta \to \infty,$$

$$\Rightarrow \theta(\infty) \to 0.$$

3.5 Dimensionless form of Skin Friction and Nusselt Number

The definition of local skin friction and local Nusselt number Nu_x are

$$C_{fx} = \frac{1}{\rho_{nf} u_w^2} \left((\mu_{nf} + \kappa) \frac{\partial u}{\partial y} + \kappa N \right)_{\eta=0}.$$

$$\Rightarrow C_{fx} = \frac{1}{((1-\phi)\rho_f + \phi\rho_s)\, x^2 F'(\eta)^2} \left[\left(\frac{\mu_f}{(1-\phi)^{2.5}} + K\mu_f axF''(\eta) \sqrt{\frac{a}{\nu_f}} \right) + K\mu_f.ax \sqrt{\frac{a}{\nu_f}} G(\eta) \right]_{\eta=0},$$

$$\Rightarrow Re_x^{\frac{1}{2}} C_{fx} = \frac{Re_x^{\frac{1}{2}}}{((1-\phi)\rho_f + \phi\rho_s)\, x^2 F'(\eta)^2} \left[\left(\frac{\mu_f}{(1-\phi)^{2.5}} + K\mu_f \right) axF''(\eta) \sqrt{\frac{a}{\nu_f}} + K\mu_f.ax \sqrt{\frac{a}{\nu_f}} G(\eta) \right]_{\eta=0}.$$

$$Re_x^{\frac{1}{2}} C_{fx} = \frac{ax^2\sqrt{\frac{a}{\nu_f}}}{\left((1-\phi)\rho_f + \phi\rho_s\right)x^2F'(\eta)^2}\Bigg[\left(\frac{\mu_f}{(1-\phi)^{2.5}} + K\mu_f\right)F''(\eta)\sqrt{\frac{a}{\nu_f}} + K\mu_f\sqrt{\frac{a}{\nu_f}}G(\eta)\Bigg]_{\eta=0},$$

$$\Rightarrow Re_x^{\frac{1}{2}} C_{fx} = \mu_f\frac{ax^2\sqrt{\frac{a}{\nu_f}}}{\left((1-\phi)\rho_f + \phi\rho_s\right)x^2F'(\eta)^2}\Bigg[\left(\frac{1}{(1-\phi)^{2.5}} + K\right)F''(\eta)\sqrt{\frac{a}{\nu_f}} + K\sqrt{\frac{a}{\nu_f}}G(\eta)\Bigg]_{\eta=0}.$$

$$\Rightarrow Re_x^{\frac{1}{2}} C_{fx} = \mu_f\frac{ax^2\frac{a}{\nu_f}}{\left((1-\phi)\rho_f + \phi\rho_s\right)x^2F'(\eta)^2}\Bigg[\left(\frac{1}{(1-\phi)^{2.5}} + K\right)F''(\eta) + KG(\eta)\Bigg]_{\eta=0}.$$

$$\Rightarrow Re_x^{\frac{1}{2}} C_{fx} = \frac{a^2x^2\frac{\mu_f}{\nu_f}}{\left((1-\phi)\rho_f + \phi\rho_s\right)x^2F'(\eta)^2}\Bigg[\left(\frac{1}{(1-\phi)^{2.5}} + K\right)F''(\eta) + KG(\eta)\Bigg]_{\eta=0}.$$

$$\Rightarrow Re_x^{\frac{1}{2}} C_{fx} = \frac{a^2x^2\frac{\mu_f}{\nu_f}}{\rho_f\left((1-\phi) + \phi\frac{\rho_s}{\rho_f}\right)x^2F'(\eta)^2}\Bigg[\left(\frac{1}{(1-\phi)^{2.5}} + K\right)F''(\eta) + KG(\eta)\Bigg]_{\eta=0}.$$

$$\Rightarrow Re_x^{\frac{1}{2}} C_{fx} = \frac{a^2x^2}{\left((1-\phi) + \phi\frac{\rho_s}{\rho_f}\right)x^2F'(\eta)^2}\Bigg[\left(\frac{1}{(1-\phi)^{2.5}} + K\right)F''(\eta) + KG(\eta)\Bigg]_{\eta=0}.$$

$$\Rightarrow Re_x^{\frac{1}{2}} C_{fx} = \frac{a^2x^2}{\left((1-\phi) + \phi\frac{\rho_s}{\rho_f}\right)x^2F'(\eta)^2}\Bigg[\left(\frac{1}{(1-\phi)^{2.5}} + K\right)F''(\eta) + KG(\eta)\Bigg]_{\eta=0}.$$

$$\Rightarrow Re_x^{\frac{1}{2}} C_{fx} = \frac{1}{\left((1-\phi) + \phi\frac{\rho_s}{\rho_f}\right)}\Bigg[\left(\frac{1}{(1-\phi)^{2.5}} + K\right)F''(\eta) + KG(\eta)\Bigg]_{\eta=0}.$$

$$\Rightarrow Re_x^{\frac{1}{2}} C_{fx} = \frac{1}{\left(1-\phi + \phi\frac{\rho_s}{\rho_f}\right)}\left[\frac{1}{(1-\phi)^{2.5}} + KF''(0) - K\delta F''(0)\right].$$

$$\Rightarrow Re_x^{\frac{1}{2}} C_{fx} = \frac{1}{\left(1-\phi + \phi\frac{\rho_s}{\rho_f}\right)}\left[\frac{1}{(1-\phi)^{2.5}} + (1-\delta)K\right]F''(0).$$

By the definition of the local Nusselt number,

$$Nu_x = -\frac{x}{T_w - T_\infty}\left(\frac{\partial T}{\partial y}\right)_{y=0}.$$

$$Nu_x = -\frac{x}{T_w - T_\infty}\left(T_w - T_\infty\right)\theta'(0)\sqrt{\frac{a}{\nu_f}}.$$

$$\Rightarrow Re_x^{\frac{-1}{2}} Nu_x = -xRe_x^{\frac{-1}{2}}\theta'(0)\sqrt{\frac{a}{\nu_f}}.$$
$$\Rightarrow Re_x^{\frac{-1}{2}} Nu_x = -\frac{x}{x}\sqrt{\frac{\nu_f}{a}}\theta'(0)\sqrt{\frac{a}{\nu_f}}.$$
$$\Rightarrow Re_x^{\frac{-1}{2}} Nu_x = -\theta'(0). \tag{3.40}$$

3.6 Numerical Method for Solution

The shooting technique is used to solve the ordinary differential equations system (3.35) and (3.36). To achieve the numerical solution, the unbounded domain $[0,\infty[$ has been replaced by the bounded domain $[0,\eta_\infty]$ where η_∞ is a suitable real number having the property that there is no significant variation in the solution for $\eta > \eta_\infty$.

$$F = f_1, \quad F' = f_1' = f_2, \quad F'' = f_1'' = f_2' = f_3, \quad F''' = f_3', \quad G = f_4,$$
$$G' = f_4' = f_5, \quad G'' = f_5',$$
$$H_1 = (1-\phi)^{2.5}, \quad H_2 = H_1 + K, \quad H_3 = 1 - \phi + \phi\frac{\rho_s}{\rho_f},$$
$$H_4 = 1 + \frac{3(\sigma-1)\phi}{\sigma + 2 - (\sigma-1)\phi}, \quad H_5 = H_1 + \frac{K}{2}.$$

As a result, the momentum equation (3.35) is converted into the following system of first order ODEs.

$$f_1' = f_2, \qquad f_1(0) = \alpha,$$
$$f_2' = f_3, \qquad f_2(0) = s,$$
$$f_3' = \frac{1}{H_2}(-H_3 f_1 f_3 + H_3 f_2^2 + M H_4 f_2 - K f_5), \qquad f_3(0) = S,$$
$$f_4' = f_5 \qquad f_4(0) = -\delta S,$$
$$f_5' = \frac{1}{H_5}(-H_3 f_1 f_5 + H_3 f_2 f_4 + k(2f_4 + f_3)) \qquad f_5(0) = r.$$

The above IVP will be numerically solved by the RK-4 method. The missing conditions are to be chosen such that:

$f_2(s,r) = 0, \quad f_4(s,r) = 0,$

which are the values of f_2 and f_4 at η=η_∞ for the missing initial conditions (s,r). Newton's method will be used to solve the above algebraic equations.This method has the following iterative scheme:

$$\begin{bmatrix} s^{n+1} \\ r^{n+1} \end{bmatrix} = \begin{bmatrix} s^{n} \\ r^{n} \end{bmatrix} - \begin{bmatrix} \frac{\partial f_2}{\partial s} & \frac{\partial f_2}{\partial r} \\ \frac{\partial f_4}{\partial s} & \frac{\partial f_4}{\partial r} \end{bmatrix}^{-1}_{(s^n,r^n)} \begin{bmatrix} f_2 \\ f_4 \end{bmatrix}_{(s^n,r^n)} \tag{3.41}$$

We further introduce the following notations.

$$\begin{aligned} &\frac{\partial f_1}{\partial s} = f_6, \quad \frac{\partial f_2}{\partial s} = f_7, \quad \frac{\partial f_3}{\partial s} = f_8 \quad \frac{\partial f_4}{\partial s} = f_9, \quad \frac{\partial f_5}{\partial s} = f_{10}, \\ &\frac{\partial f_1}{\partial r} = f_{11}, \quad \frac{\partial f_2}{\partial r} = f_{12}, \quad \frac{\partial f_3}{\partial r} = f_{13}, \quad \frac{\partial f_4}{\partial r} = f_{14}, \quad \frac{\partial f_5}{\partial r} = f_{15}, \end{aligned}$$

As a result of these new notations, the Newton's iterative scheme get the form:

$$\begin{bmatrix} s^{n+1} \\ r^{n+1} \end{bmatrix} = \begin{bmatrix} s^{n} \\ r^{n} \end{bmatrix} - \begin{bmatrix} f_7 & f_{12} \\ f_9 & f_{14} \end{bmatrix}^{-1}_{(s^n,r^n)} \begin{bmatrix} f_2 \\ f_4 \end{bmatrix}_{(s^n,r^n)}. \tag{3.42}$$

Now differentiating the last system of five first order ODEs with respect to s and r, we get another system of ODEs, which has been presented below.

$$\begin{aligned} f_6' &= f_7, & f_6(0) &= 0, \\ f_7' &= f_8, & f_7(0) &= 0, \\ f_8' &= \frac{1}{H_2}(-H_3 f_1 f_8 - H_3 f_3 f_6 + 2H_3 f_2 Q_7 + M H_4 f_7 - K f_{10}), & f_8(0) &= 1, \\ f_9' &= f_{10}, & f_9(0) &= 0, \\ f_{10}' &= \frac{1}{H_5}(-H_3 f_1 f_5 - H_3 f_5 f_6 + H_3 f_2 f_9 + H_3 f_4 f_7 + k(2f_9 + f_8)) & f_{10}(0) &= 0, \\ f_{11}' &= f_{12} & f_{11}(0) &= 0, \\ f_{12}' &= f_{13} & f_{12}(0) &= 0, \\ f_{13}' &= \frac{1}{H_2}(-H_3 f_1 f_{13} - H_3 f_3 f_{11} + 2H_3 f_2 f_{12} + M H_4 f_{12} - K f_{15}) & f_{13}(0) &= 0, \\ f_{14}' &= f_{15} & f_{14}(0) &= 0, \end{aligned}$$

$$f'_{15} = \frac{1}{H_5}(-H_3 f_1 f_{15} - H_3 f_5 f_{11} + H_3 f_2 f_{14} + H_3 f_4 f_{12} + k(2f_{14} + f_{13})) \qquad f_{15}(0) = 1.$$

The stopping criteria for the Newton's technique is set as

$$max\{|f_2(\eta_\infty, s^n, r^n)|, |f_4(\eta_\infty, s^n, r^n)|\} < \epsilon,$$

where $\epsilon > 0$ is an arbitrarily small positive number. From now onward, ϵ has been taken as 10^{-10}.

The equation (3.37) will also be numerically solved by using the shooting method. For this, we utilize the following notions:

$$\theta = Y_1, \qquad \theta' = Y_2, \qquad \theta'' = Y_2'.$$
$$H_6 = \frac{\left(\frac{\kappa_s + 2\kappa_f - 2\phi(\kappa_f - \kappa_s)}{\kappa_s + 2\kappa_f + \phi(\kappa_f - \kappa_s)} + R\right)}{Pr}, \qquad H_7 = 1 - \phi + \phi\frac{(\rho Cp)_s}{(\rho Cp)_f}, \qquad H_1 = \frac{1}{(1-\phi)^{2.5}}.$$

As a result, the energy equation (3.37) is converted into the following system of first order ODEs.

$$\begin{aligned} Y_1' &= Y_2, & Y_1(0) &= 1, \\ Y_2' &= \frac{1}{H_6}\left(-H_7 F(\eta) Y_2\right), & Y_2(0) &= l. \end{aligned}$$

The above initial value problem will be numerically solved by RK-4 technique. In this problem, the missing condition is l and it satisfies the following relation.

$$Y_1(l) = 0,$$

where $Y_1(l)$ is the value of Y_1 at $\eta = \eta_\infty$ for the missing initial condition l. The Newton's iterative scheme gets the form,

$$l^{n+1} = l^n - \frac{Y_1(\eta_\infty, l)}{\frac{\partial Y_1}{\partial l}(\eta_\infty, l)}.$$

We further introduce the following notations,

$$\frac{\partial Y_1}{\partial l} = Y_3, \qquad \frac{\partial Y_2}{\partial l} = Y_4.$$

As a result of these new notations, the Newton's iterative scheme gets the form:

$$l^{n+1} = l^n - \frac{Y_1(l^n)}{Y_3(l^n)}.$$

Now differentiating the last system of two first order ODEs with respect to l, we get two more ODEs.

$$\begin{aligned} Y_3' &= Y_4, & Y_3(0) &= 0, \\ Y_4' &= \frac{1}{H_6}\left(-H_7 F(\eta) Y_4\right), & Y_4(0) &= 1. \end{aligned}$$

The stopping criteria for the Newton's method is set as:

$$\mid Y_1(\eta_\infty, l) \mid < \epsilon.$$

3.7 Numerical Results

Tiwari-Das model is used to analyze boundary layer flow and heat transfer of a micro polar magnetite ferro fluid over a stretching and shrinking sheet under the effect of thermal radiation. The effects of parameters like suction/injection, radiation, magnetic, micro rotation, boundary parameters and Prandtl number on $F'(\eta)$, G(η), $\theta(\eta)$ are analyzed for stretching and shrinking cases, separately. A thorough discussion on the graphs and tables has been conducted which contains the impact of dimensionless parameters on the local skin friction coefficient $(Re_x)^{\frac{1}{2}} C_{fx}$ and local Nusselt number $(Re_x)^{\frac{-1}{2}} Nu_x$. Table 3.1 explains the impact of different parameters on the skin friction. For the rising values of ϕ, the skin friction coefficient decreases. It is evident that with an increase in the micro rotation parameter K, the skin friction coefficient increases. By increasing the values of ϕ, M, S, α and δ, the skin friction coefficient is decreased. In Table 3.2, the effects of significant parameters on Nusselt number $(Re_x)^{\frac{-1}{2}} Nu_x$ has been discussed. The rising pattern is found in $(Re_x)^{\frac{-1}{2}} Nu_x$ due to an increase in values of the rotation parameter K, suction/injection and boundary parameter δ. The value of Nusselt

number decreases as we increase the value of M, ϕ and radiation parameter R. In table 3.1 and 3.2 the missing conditions are taken from the intervals represented by s and t and w.

Figures 3.1 and 3.2 show the velocity profile for different values of M in case of suction and injection. The graph show that if we increase the values of M, the velocity $F'(\eta)$ decreases for both the cases. The Lorentz force, also called the drag force which is immediately increased by increasing M plays very vital role to maintain the fluid motion slow. It is evident that a pointy fall within the pace for $S > 0$ compared to $S < 0$ inside the layer $eta < 4$ and then after it will become uniform.

Figures 3.3 and 3.4 show the impact of the magnetic parameter M on the velocity profile for injection and suction when $\alpha < 0$ (shrinking case). It depicts that for mass transfer flow the velocity profile is a decreasing function of M. Also in Figures 3.5 and 3.6, it can be noted that if we increase the value of K in case of injection and suction, the velocity profile is significantly increased.

Figures 3.7 and 3.8 describe the effect of micro rotation parameter K on the velocity field $F'(\eta)$ in case of suction. It is noted that an increment in the value of K results in increasing the magnitude of the velocity profile. The same can be seen for the injection case. The boundary layer thickness is greater for the injection case while it is less for the case of suction when the other parameters are kept constant.

In Figure 3.9, we have the velocity profile for suction and stretching for different values of δ. It can be seen clearly that with an increase in the value of δ, the velocity of the fluid decreases for the case of suction and stretching. In Figure 3.10, we have the velocity profile for injection and stretching for different values of δ. It can be seen clearly that with an increase in the value of δ, the velocity of the fluid decreases for the cases of injection and stretching. In case of $\delta = 0$, the stretching sheet is not easy to rotate and shows low concentration. The stress tensor is vanished for value of $\delta = \frac{1}{2}$ and it reflects low concentration of micro elements and for turbulent flow the value of $\delta = 1$.

The impacts of δ for suction and injection are displayed in Figures 3.11 and 3.12.It is notable that δ significantly affects the velocity profile and causes a decrement in

the velocity magnitude. Deceleration in the velocity boundary layer as compared with the injection case is zero.

Figures 3.13 and 3.14 illustrate the impact of M on the micro rotation profile. It is observed that the magnitude of the micro rotation velocity increases with an increase in the magnetic field parameter M while on the other hand, micro rotation velocity increases by increasing M. Figure 3.15 represent the variations in the micro rotation velocity for suction and shrinking and Figure 3.16 represents the variation in the micro rotation velocity for injection and shrinking.

Figure 3.17 gives the temperature distribution in case of suction and stretching for different values of R. It is clear that a rise in R also rises the temperature. So the heat transfer is increased with a rise in the value of R. Figure 3.18 shows the temperature distribution in case of injection for different values of R for injection and stretching. This graph also indicates that for micro-polar ferro fluid, the rate of heat transfer is high as compared to that for the micro-polar fluid.

Figures 3.19 and 3.20 describe the temperature distribution for suction and stretching by taking different values of R. The increasing value of R is taken out in both cases for micro polar ferro fluid and nanofluid as well. It is clear that a rise in R and the percentage of nano particles in the base fluid will increase the rate of flow of heat. It is also observed that a rise in R and the percentage of nano particles in the base fluid will increase the flow of heat transfer for suction and injection case.

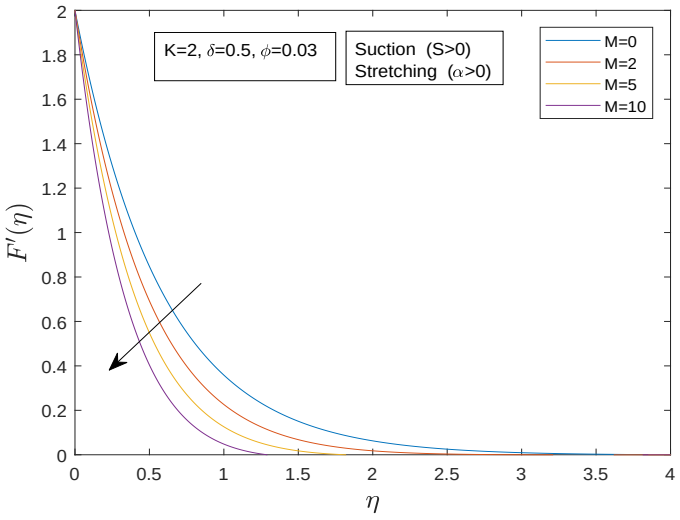

FIGURE 3.1: Impact of M on velocity profile for Injection and stretching.

TABLE 3.1: Results of $Re^{\frac{1}{2}}Cf_x$ for various parameters

ϕ	K	M	S	α	δ	$Re^{\frac{1}{2}}Cf_x$	s	t
0.01	0.2	0.4	0.5	0.5	0.5	-0.613253	[-1,1]	[-1,2]
0.05						-0.765462	[-0.4,5]	[-0.4,4]
0.1						-0.999178	[-0.9,10]	[-5,5]
0.2						-1.655136	[-0.9,10]	[-5,5]
	2					-0.451792	[1,10]	[-5,-0.1]
	3					-0.410157	[-1,8]	[-5,-0.1]
	4					-0.382136	[-0.9,0.7]	[-5,1]
	5					-0.362282	[-1.3,5]	[-5,1]
		2				-0.913687	[-1.3,5]	[-5,5]
		4				-1.172478	[-1,5]	[-5,5]
		6				-1.377868	[-1.3,4]	[-5,5]
		8				-1.553499	[-1.3,1]	[-5,5]
			1			-0.777384	[-1.1,5]	[-5,5]
			2			-1.165519	[-1.9,10]	[-5,5]
			3			-1.598276	[-3,3]	[-5,5]
			4			-2.052235	[-4,4]	[-5,5]
				5		-12.98383	[-5,5]	[-5,5]
				6		-16.82282	[-5,4]	[-5,5]
				7		-20.96724	[-5,1]	[-5,5]
				7.2		-21.830737	[-5,0]	[-5,5]
					0.1	-0.590222	[0,10]	[-5,3]
					0.3	-0.601494	[0,10]	[-5,3]
					0.5	-0.613253	[-5,5]	[-5,5]
					0.9	-0.638371	[0,10]	[-5,5]
					1	-1.590222	[0,10]	[-5,3]
					3	-2.601494	[0,10]	[-5,3]
					5	-3.613253	[-5,5]	[-5,5]
					9	-4.638371	[0,10]	[-5,5]

TABLE 3.2: Results of $-(Re_x^{\frac{-1}{2}})Nu_x$ for various parameters

ϕ	K	M	S	α	R	δ	$-(Re_x^{\frac{-1}{2}})Nu_x$	s	t	w
0.01	0.2	0.4	0.5	0.5	0.7	0.5	2.281019	[1,10]	[-5,4]	[-10,10]
0.05							2.150160	[-0.7,10]	[-5,5]	[-10,10]
0.1							1.997185	[-0.9,10]	[-5,5]	[-10,10]
0.2							1.722660	[-0.9,10]	[-5,5]	[-10,10]
	1						2.301144	[-0.9,10]	[-5,4]	[-10,10]
	2						2.316742	[-0.9,5]	[-5,0]	[-10,10]
	3						2.326982	[-1,5]	[-5,1]	[-10,10]
	4						2.334257	[-1,5]	[-5,1]	[-10,10]
		2					2.226615	[-1,5]	[-5,5]	[-10,10]
		4					2.186344	[-1,5]	[-5,5]	[-10,10]
		5					2.171452	[-1.3,5]	[-5,5]	[-10,10]
		8					2.137106	[-1.3,1.3]	[-5,5]	[-10,10]
			1				3.910179	[-1.3,5]	[-5,5]	[-10,10]
			2				7.361208	[-1.3,5]	[-5,5]	[-10,10]
			3				10.892073	[-1.3,5]	[-5,5]	[-10,10]
			4				14.449370	[-1.3,5]	[-5,5]	[-10,10]
				0			1.795305	[-0.1,5]	[-5,5]	[-10,10]
				1			2.613540	[-1.3,5]	[-5,5]	[-10,10]
				2			3.115141	[-1.3,5]	[-5,5]	[-10,10]
				3			3.511772	[-1.3,5]	[-5,5]	[-10,10]
					1		1.983329	[-0.1,5]	[-5,3]	[-10,10]
					2		1.352791	[-1.3,5]	[-5,5]	[-10,10]
					3		1.400985	[-0.1,5]	[-5,5]	[-10,10]
					4		0.912845	[-0.1,5]	[-5,4]	[-10,10]
						0.1	2.285946	[-1.3,5]	[-5,5]	[-10,10]
						0.3	2.283545	[-1.3,5]	[-5,5]	[-10,10]
						0.5	2.281019	[-1.3,5]	[-5,5]	[-10,10]
						0.9	2.275547	[-1.3,5]	[-5,5]	[-10,10]

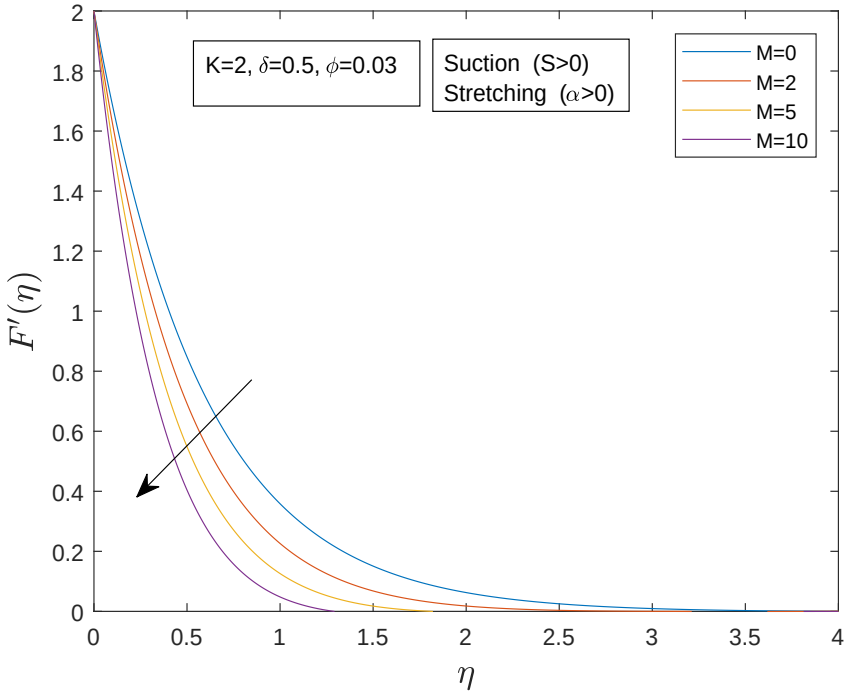

FIGURE 3.2: Impact of M on velocity profile for Injection and stretching.

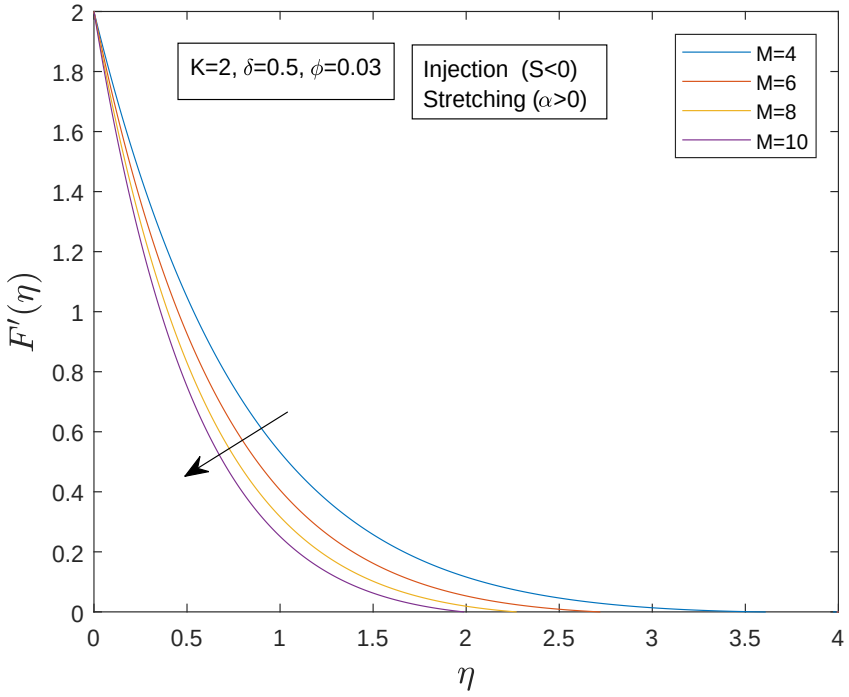

FIGURE 3.3: Impact of M on velocity profile for Injection and stretching.

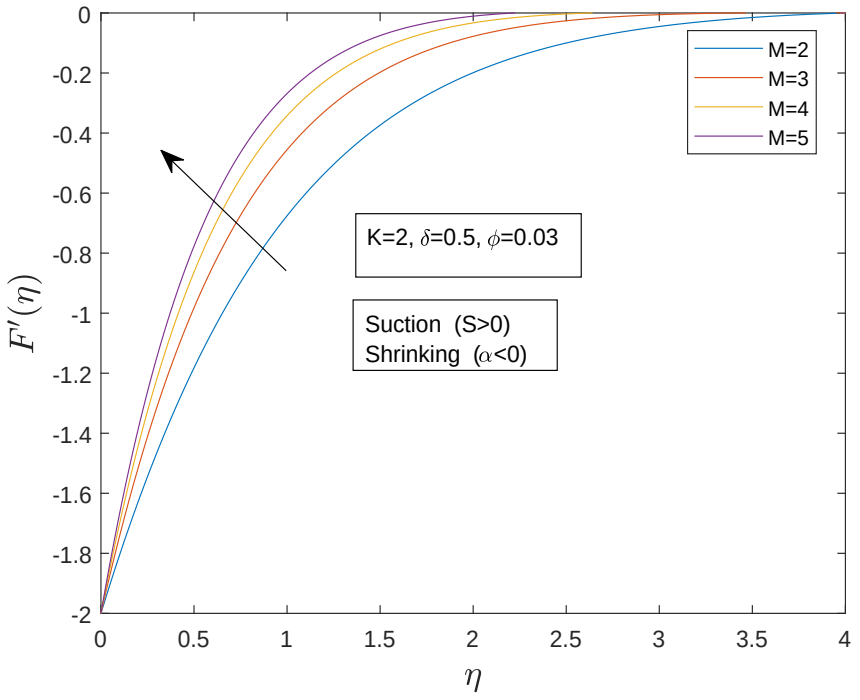

FIGURE 3.4: Impact of M on velocity profile for suction and shrinking.

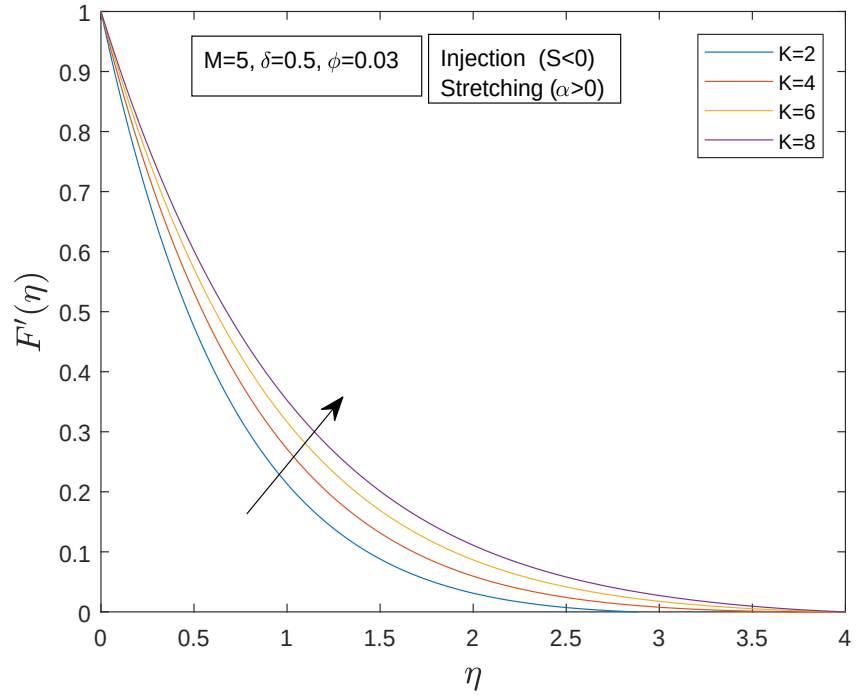

FIGURE 3.5: Impact of K on velocity profile for stretching and injection.

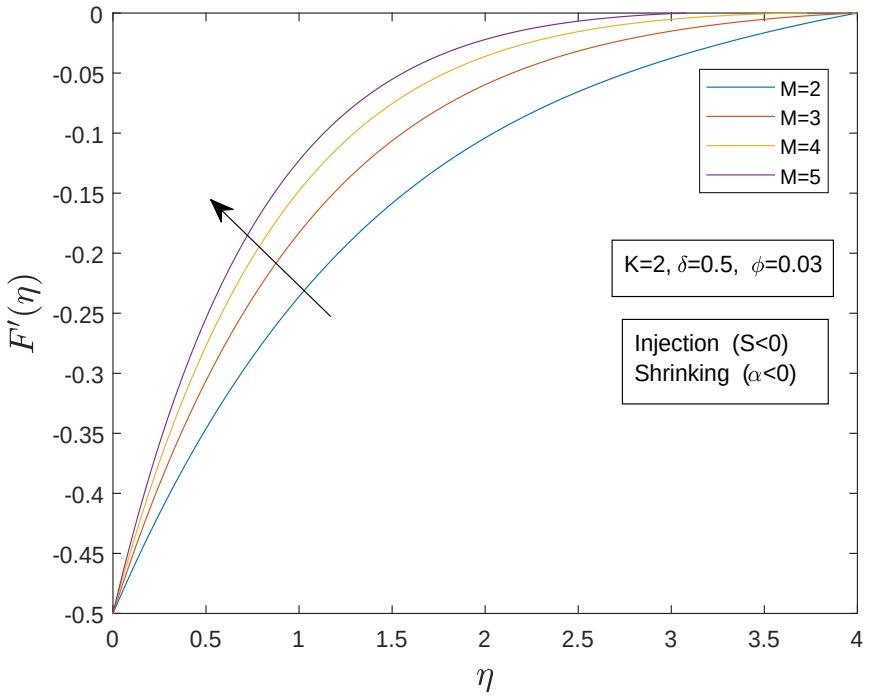

FIGURE 3.6: Impact of M on velocity profile for shrinking and injection.

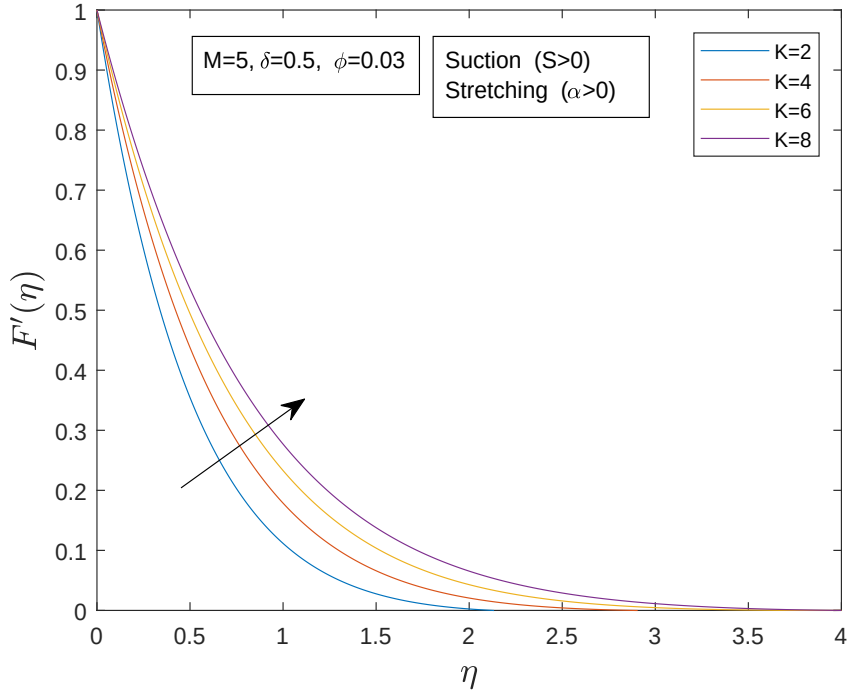

FIGURE 3.7: Impact of K on velocity profile for suction and stretching.

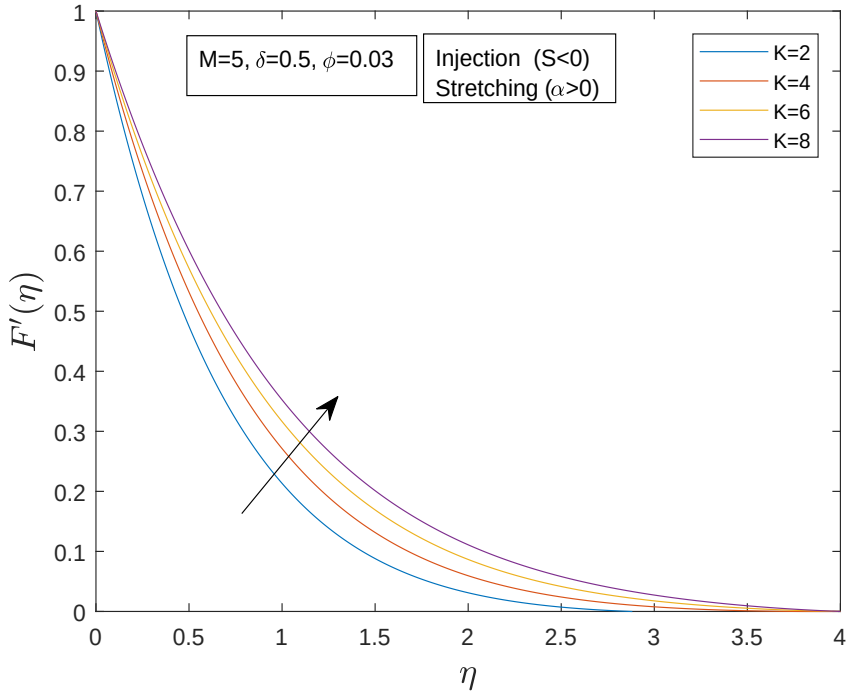

FIGURE 3.8: Impact of K on velocity profile for stretching and injection.

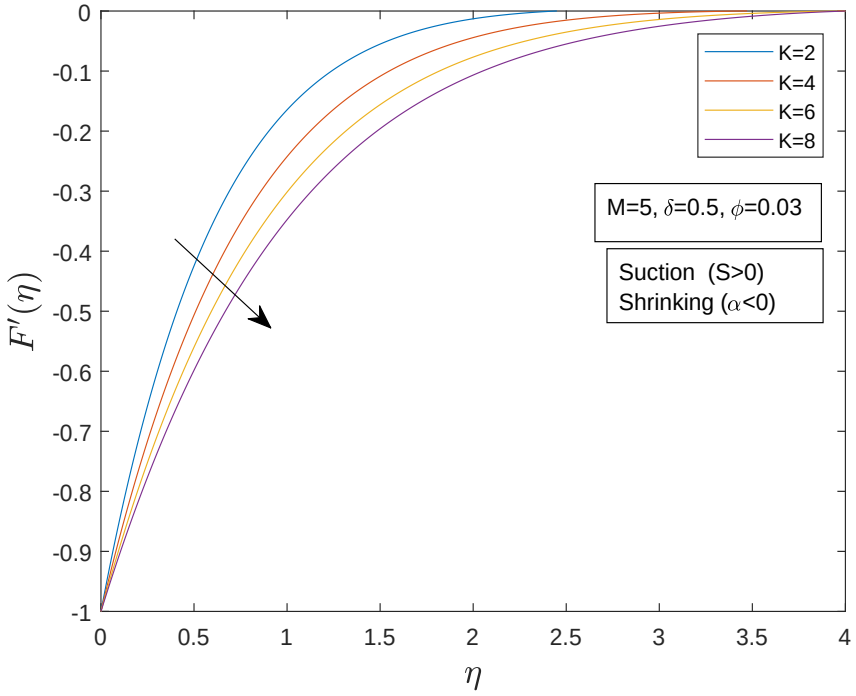

FIGURE 3.9: Impact of K on velocity profile for suction and shrinking.

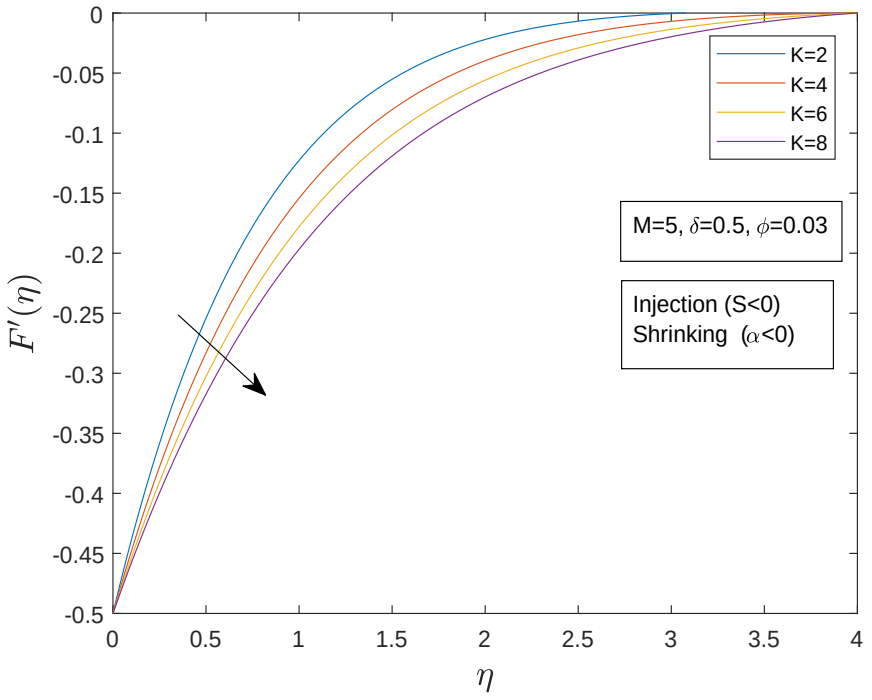

FIGURE 3.10: Impact of K on velocity profile for shrinking and injection.

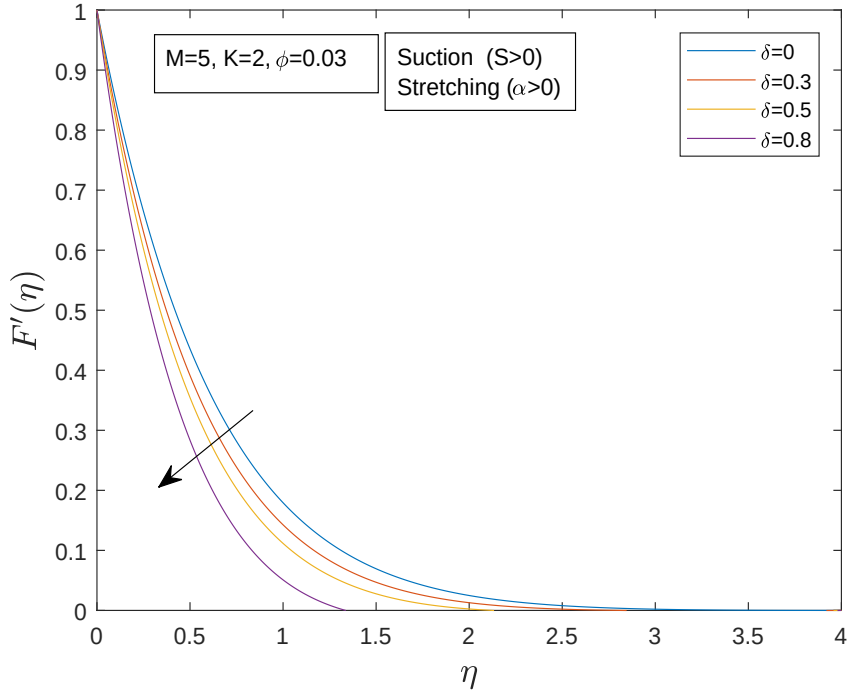

FIGURE 3.11: Impact of δ on velocity profile for stretching and suction.

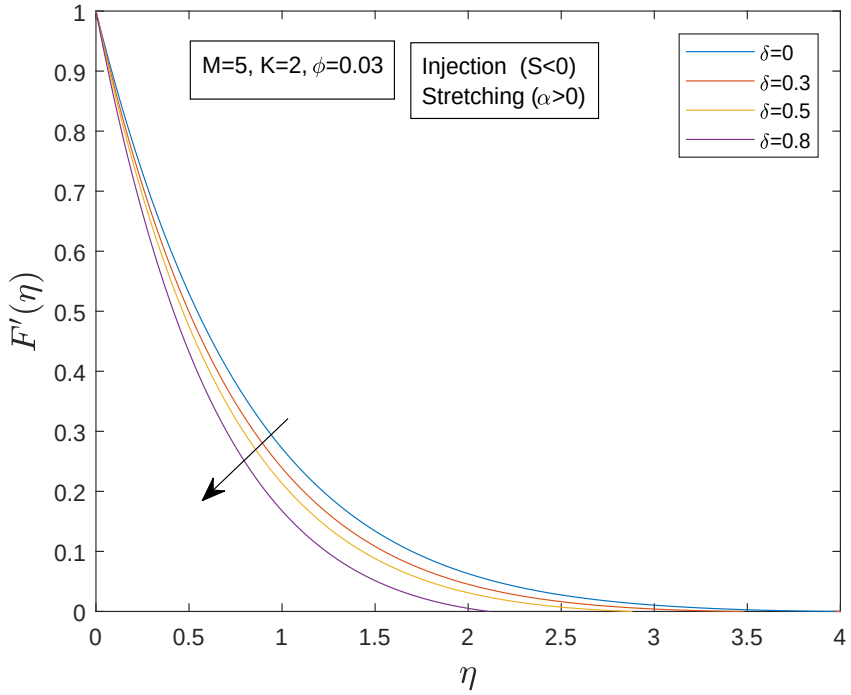

FIGURE 3.12: Impact of δ on velocity profile for stretching and injection.

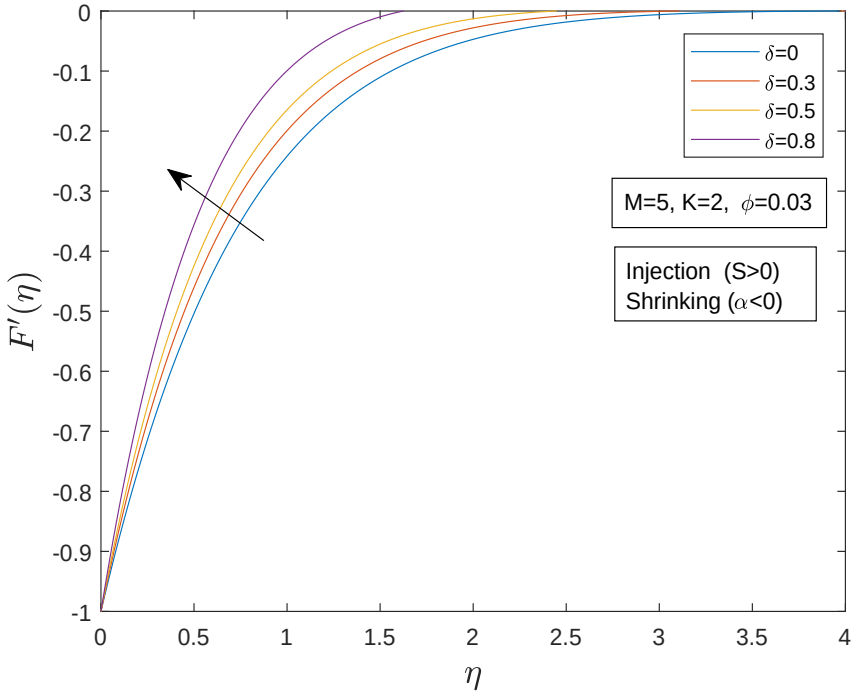

FIGURE 3.13: Impact of δ on velocity profile for shrinking and suction.

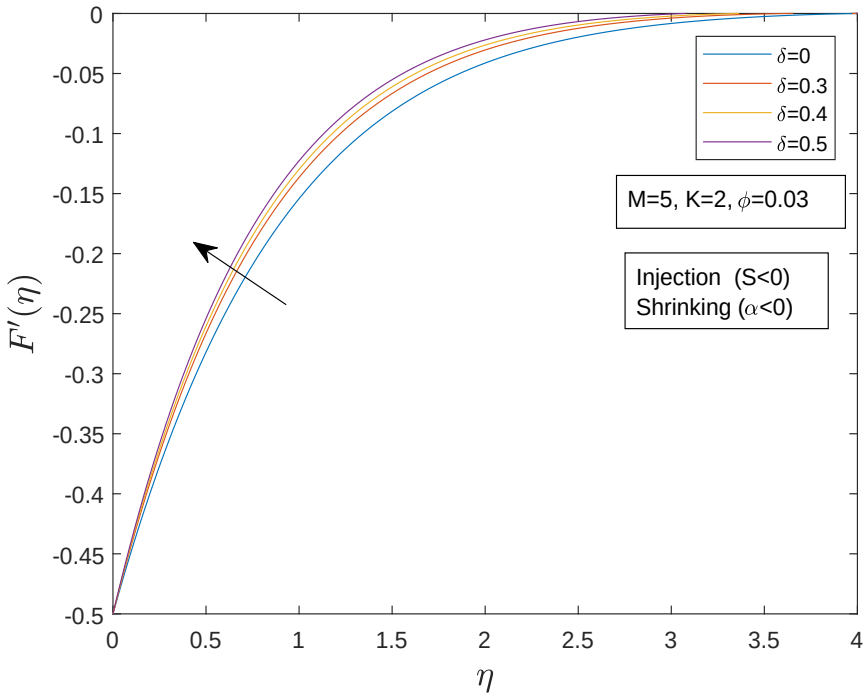

FIGURE 3.14: Impact of δ on velocity profile for shrinking and injection.

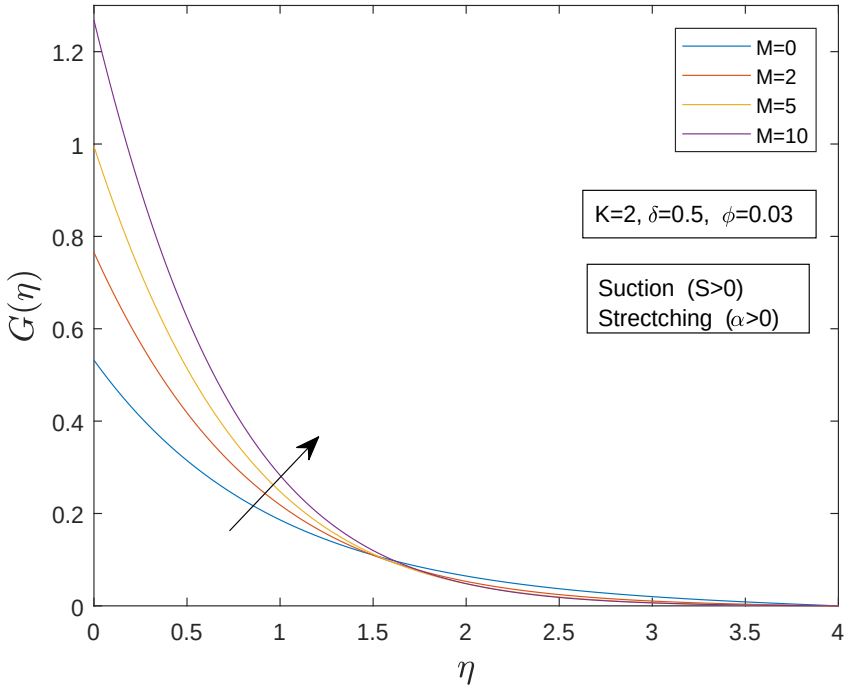

FIGURE 3.15: Impact of M on micro rotation velocity profile for suction and stretching.

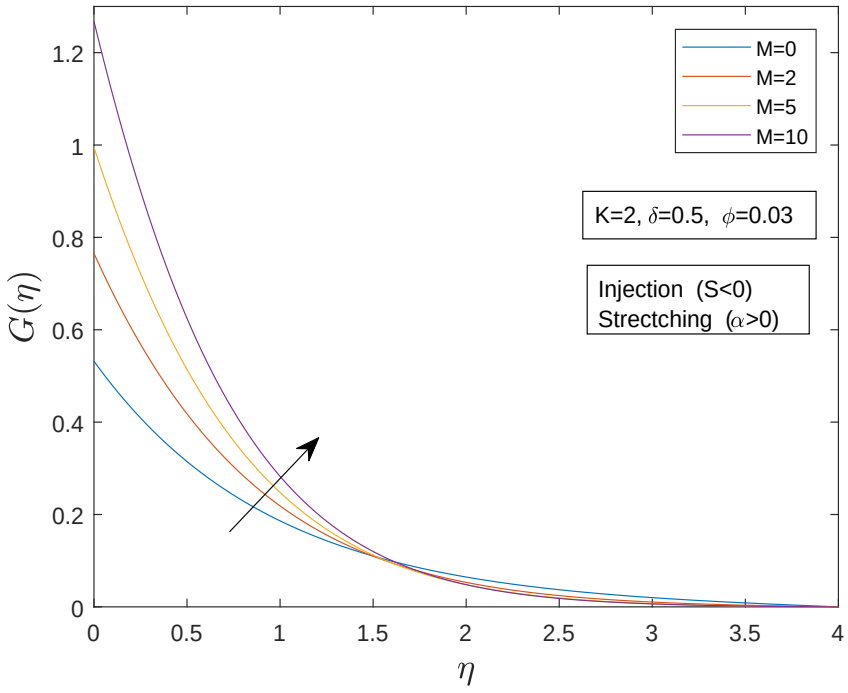

FIGURE 3.16: Impact of M on micro rotation velocity profile for stretching and injection.

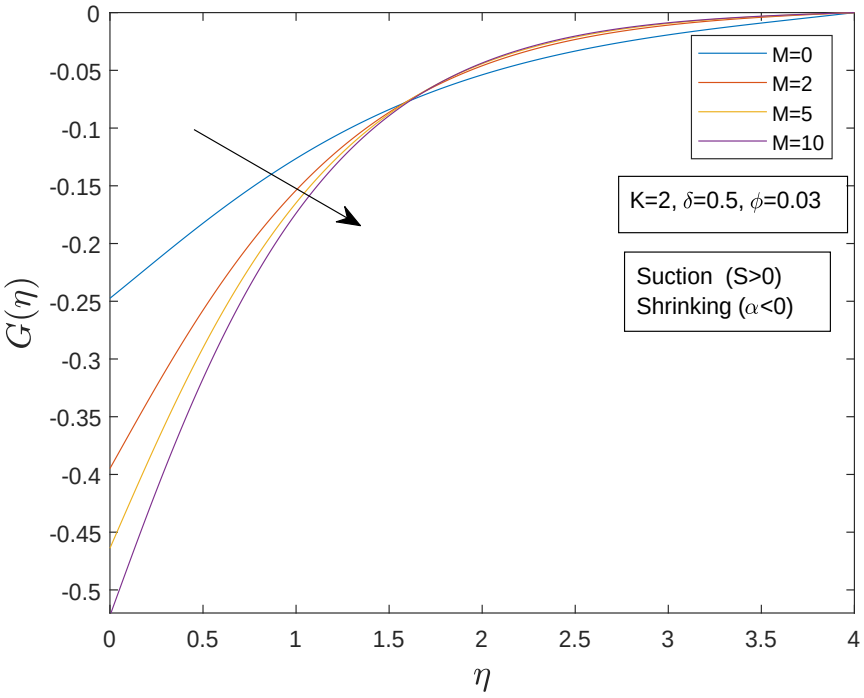

FIGURE 3.17: Impact of M on micro rotation velocity for suction and shrinking.

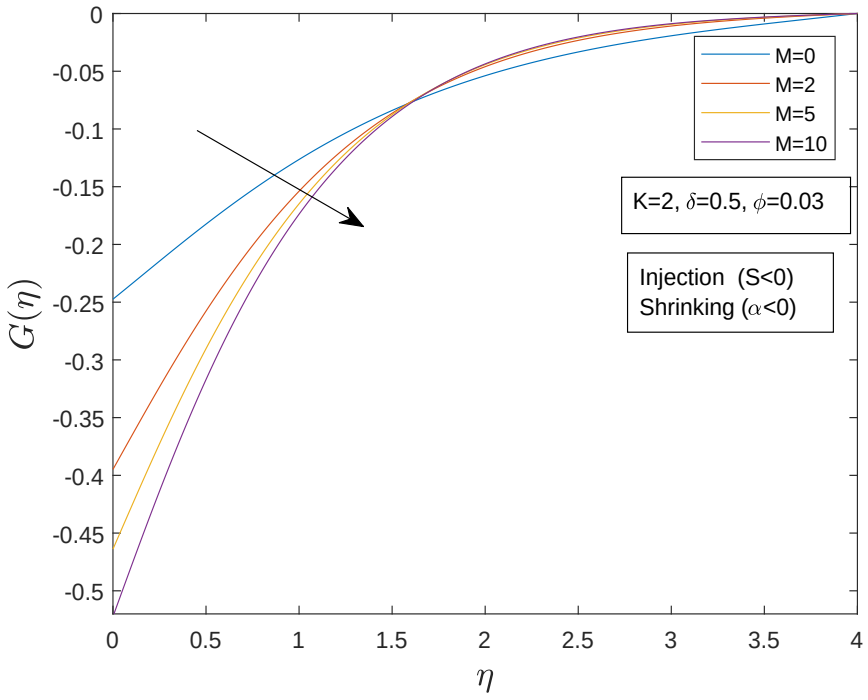

FIGURE 3.18: Impact of M on micro rotation velocity profile for shrinking and injection.

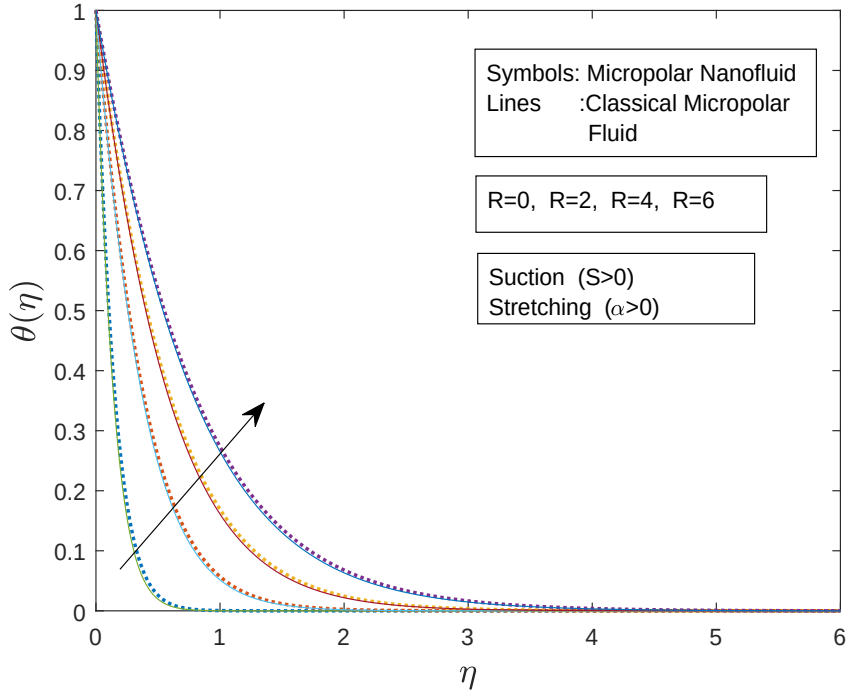

FIGURE 3.19: Comparison of temperature field between micro polar and classical fluid for suction and stretching.

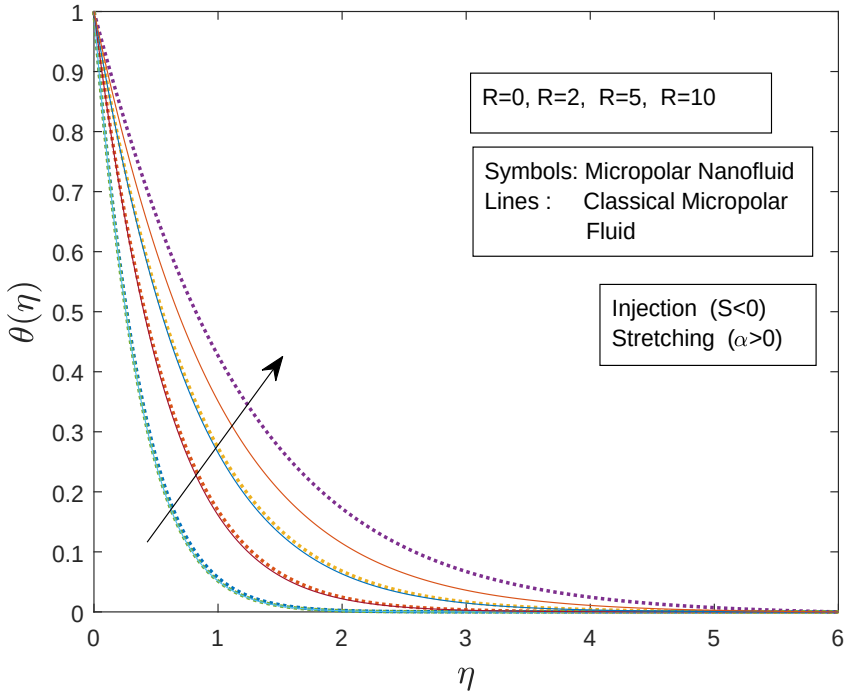

FIGURE 3.20: Comparison of temperature field between micro polar and classical fluid for injection and stretching.

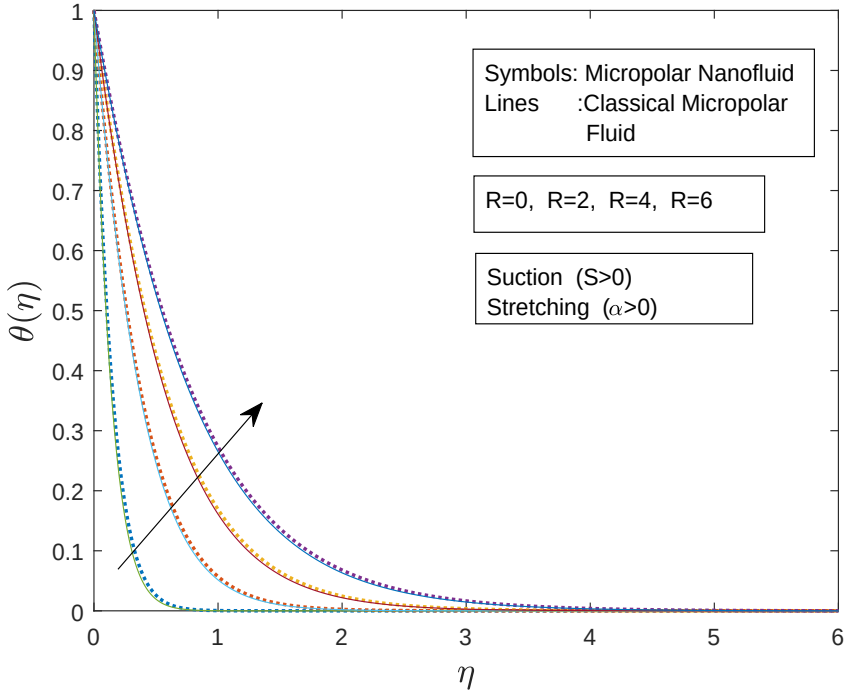

FIGURE 3.21: Comparison of temperature field between micro polar and classical fluid for suction and stretching.

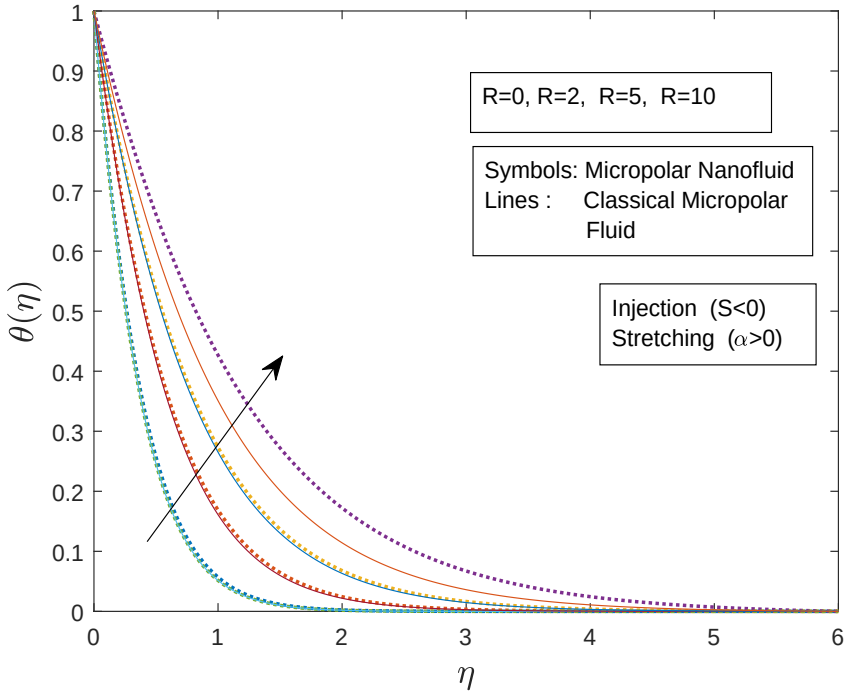

FIGURE 3.22: Comparison of temperature field between micro polar and classical fluid for Injection and stretching.

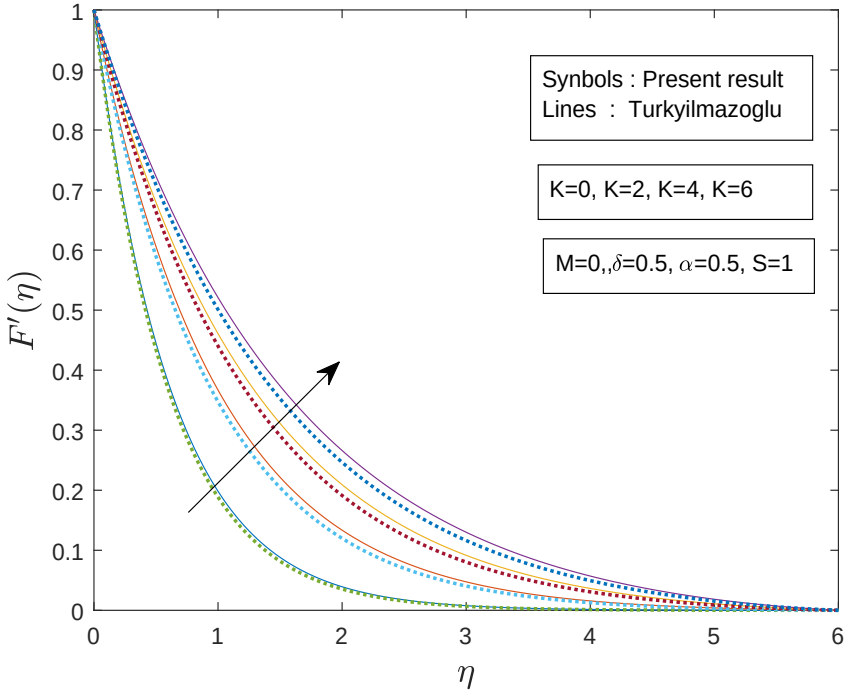

FIGURE 3.23: Comparison of temperature field between micro polar and classical fluid for different values of K.

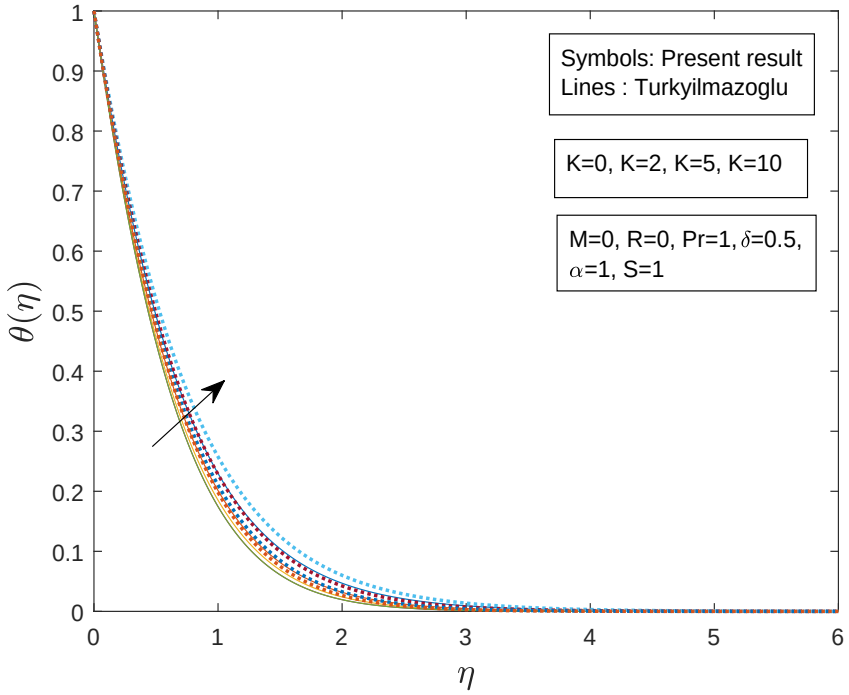

FIGURE 3.24: Comparison of temperature field between micro polar and classical fluid for different values of K.

Chapter 4

Numerical Study of Viscous Dissipation and Catteno Christov Heat Flux

4.1 Introduction

The numerical analysis of a nanofluid flow towards a stretching and shrinking sheet using Tiwari and Das [13] conductivity model and Cattaneo-Christov heat flux, viscous dissipation has been studied in this chapter. The governing PDEs are transformed into a system of dimensionless ODEs by using an appropriate transformation. The governing non linear PDEs, are transformed into a system of dimensionless ODEs, by using similarity transformation. The reduced equation are then solved numerically with the aid of shooting method. At the end of this chapter, numerical solutions for several parameters are discussed for the dimensionless velocity and temperature distributions. The numerical results are expressed through tables and graphs.

4.2 Mathematical Modeling

A steady two-dimensional boundary layer flow of a micro-polar ferrofluid in the presence of Cattaneo-Christov heat flux and viscous dissipation. For a stretching

and shrinking case a magnetic field B_0 is applied perpendicular to the sheet and the velocity is assumed as $u_w(x) = ax$. Furthermore by using shooting technique, the solution of ODEs is obtained.

$$\frac{\partial u}{\partial x} + \frac{\partial v}{\partial y} = 0, \tag{4.1}$$

$$\rho_{nf}\left(u\frac{\partial u}{\partial x} + v\frac{\partial u}{\partial y}\right) = (\mu_{nf} + k)\frac{\partial^2 u}{\partial^2 y} + k\frac{\partial N}{\partial y} - \sigma_{nf}B^2\!\!\not{}u, \tag{4.2}$$

$$\rho nfj\left(u\frac{\partial N}{\partial x} + v\frac{\partial N}{\partial y}\right) = \gamma_{nf}\frac{\partial^2 N}{\partial^2 y} - k\left(2N + \frac{\partial u}{\partial x}\right), \tag{4.3}$$

$$\begin{aligned} u\frac{\partial T}{\partial x} + v\frac{\partial T}{\partial y} &= \frac{k_{nf}}{(\sigma c_p)_{nf}}\frac{\partial^2 T}{\partial^2 y} - \frac{\partial q_r}{\partial y} \\ &+ \lambda_2\left[u\frac{\partial u}{\partial x}\frac{\partial T}{\partial x} + v\frac{\partial v}{\partial y}\frac{\partial T}{\partial x} + u\frac{\partial v}{\partial x}\frac{\partial T}{\partial y} + v\frac{\partial u}{\partial y}\frac{\partial T}{\partial x} + 2uv\frac{\partial^2 T}{\partial x \partial y} + u^2\frac{\partial^2 T}{\partial^2 x} + v^2\frac{\partial^2 T}{\partial y^2}\right] \\ &+ \frac{\mu_{nf}}{(\rho C_p)_{nf}}\left(\frac{\partial u}{\partial y}\right)^2. \end{aligned} \tag{4.4}$$

4.3 Boundary Conditions

The associated conditions are:

$$\begin{aligned} &u = \alpha u_w(x), \quad v = v_w \quad at \quad y = 0; \quad u \to 0 \quad as\ y \to \infty, \\ &N = -\delta\frac{\partial u}{\partial y} \qquad\qquad at \quad y = 0; \quad N \to 0 \quad as \quad y \to \infty, \\ &T = T_w \qquad\qquad\quad at \quad y = 0; \quad T \to T_\infty \ \ as \ \ y \to \infty. \end{aligned}$$

where v_w is the surface mass transfer velocity and corresponds to suction for $v_w > 0$ and injection for $v_w < 0$. The parameter δ is the micro gyration vector and the value of δ varies in the interval [0,1].

4.4 Conversion of PDEs to ODEs

To convert the above partial differential equation into ordinary differential equation we will use the following transformations.

$$\eta = y\sqrt{\frac{a}{v_f}}, \quad u = axF'(\eta), \quad v = -\sqrt{av_f}F(\eta), \quad N = ax\sqrt{\frac{a}{v_f}}G(\eta),$$
$$\theta(\eta) = \frac{T - T_\infty}{T_w - T_\infty}.$$

Here T_w and T_∞ are the temperatures at the wall and close to the other end of the boundary layer respectively.

The Eckert number is given by

$$E_c = \frac{a^2x^2(C_p)_f}{T_w - T\infty}. \tag{4.5}$$

$$\text{viscous dessipation } = \frac{\mu_{nf}}{(\rho C_p)_{nf}}\left(\frac{\partial u}{\partial y}\right)^2,$$

$$\text{viscous dessipation } = \frac{\mu_{nf}}{(\rho C_p)_{nf}}\frac{a^3x^2F''(\eta)^2}{\nu_f}. \tag{4.6}$$

The Cattaneo-christov heat flux is given by

$$\lambda_2\left(u\frac{\partial u}{\partial x}\frac{\partial T}{\partial x} + v\frac{\partial v}{\partial y}\frac{\partial T}{\partial x} + u\frac{\partial v}{\partial x}\frac{\partial T}{\partial y} + v\frac{\partial u}{\partial y}\frac{\partial T}{\partial x} + 2uv\frac{\partial^2 T}{\partial x\partial y} + u^2\frac{\partial^2 T}{\partial^2 x} + v^2\frac{\partial^2 T}{\partial y^2}\right),$$

$$= \lambda_2\left(u(aF'(\eta))(0)\right) + v\left(-aF'(\eta)\right)(0) + \left(u(0)(T_w - T_\infty)\theta'(\eta)\sqrt{\frac{a}{\nu_f}}\right)$$
$$+ vaxF''(\eta)\sqrt{\frac{a}{\nu_f}}(0) + 2uv\left((T_w - T_\infty)\theta'(\eta)\sqrt{\frac{a}{\nu_f}}\right)(0) + u^2(0)$$
$$+ v^2\left(T_w - T_\infty\right)\theta'(\eta)\frac{a}{\nu_f},$$
$$= \lambda_2\left(v^2(T_w - T_\infty)\theta'(\eta)\frac{a}{\nu_f}\right),$$
$$= \lambda_2\left(-\sqrt{a\nu_f}F(\eta)\right)2(T_w - T_\infty)\theta'(\eta)\frac{a}{\nu_f},$$
$$= \lambda_2\left(a^2F^2(\eta)\left(T_w - T_\infty\right)\theta'(\eta)\right). \tag{4.7}$$

Equation (4.4) will now, be converted into the dimensionless form as follows.

$$u\frac{\partial T}{\partial x} + v\frac{\partial T}{\partial y} = \frac{k_{nf}}{(\sigma c_p)_{nf}}\frac{\partial^2 T}{\partial^2 y} - \frac{\partial q_r}{\partial y}$$
$$+ \lambda_2\left[u\frac{\partial u}{\partial x}\frac{\partial T}{\partial x} + v\frac{\partial v}{\partial y}\frac{\partial T}{\partial x} + u\frac{\partial v}{\partial x}\frac{\partial T}{\partial y} + v\frac{\partial u}{\partial y}\frac{\partial T}{\partial x} + 2uv\frac{\partial^2 T}{\partial x\partial y} + u^2\frac{\partial^2 T}{\partial^2 x}\right.$$
$$\left. + v^2\frac{\partial^2 T}{\partial y^2}\right] + \frac{\mu_{nf}}{(\rho C_p)_{nf}}\left(\frac{\partial u}{\partial y}\right)^2,$$

$$\Rightarrow v\theta'(\eta)\left(T_w-T_\infty\right)\sqrt{\frac{a}{\nu_f}}=\frac{\kappa_f}{\left(\rho C_p\right)_{nf}}\Bigg[\frac{\kappa_s+2\kappa_f-2\phi(\kappa_f-\kappa_s)}{\kappa_s+2\kappa_f+\phi(\kappa_f-\kappa_s)}+R\Bigg]\theta''(\eta)\left(T_w-T_\infty\right)\sqrt{\frac{a}{\nu_f}}+\lambda_2\left(a^2F^2(\eta)\left(T_w-T_\infty\right)\theta'(\eta)\right)+\frac{\mu_{nf}}{\left(\rho C_p\right)_{nf}}\frac{a^3x^2F''(\eta)^2}{\nu_f}.$$

Using similarity transformations in above equation, we get

$$-\sqrt{a\nu_f}F(\eta)\theta'(\eta)\left(T_w-T_\infty\right)\sqrt{\frac{a}{\nu_f}}=\frac{\kappa_f}{\left(\rho C_p\right)_{nf}}\Bigg[\frac{\kappa_s+2\kappa_f-2\phi(\kappa_f-\kappa_s)}{\kappa_s+2\kappa_f+\phi(\kappa_f-\kappa_s)}+R\Bigg]\theta''(\eta)\left(T_w-T_\infty\right)\frac{a}{\nu_f}+\lambda_2\left(a^2F^2(\eta)\left(T_w-T_\infty\right)\theta'(\eta)\right)+\frac{\mu_{nf}}{\left(\rho C_p\right)_{nf}}\frac{a^3x^2F''(\eta)^2}{\nu_f}.$$

$$\Rightarrow -aF(\eta)\theta'(\eta)=\frac{\kappa_f}{\left(\rho C_p\right)_{nf}}\Bigg[\frac{\kappa_s+2\kappa_f-2\phi(\kappa_f-\kappa_s)}{\kappa_s+2\kappa_f+\phi(\kappa_f-\kappa_s)}+R\Bigg]\theta''(\eta)\frac{a}{\nu_f}+\lambda_2\left(a^2F^2(\eta)\theta''(\eta)\right)+\frac{\mu_{nf}}{\left(\rho C_p\right)_{nf}}\frac{a^3x^2F''(\eta)^2}{\nu_f(T_w-T_\infty)}.$$

$$\Rightarrow -F(\eta)\theta'(\eta)=\frac{\kappa_f}{\left(\rho C_p\right)_{nf}}\Bigg[\frac{\kappa_s+2\kappa_f-2\phi(\kappa_f-\kappa_s)}{\kappa_s+2\kappa_f+\phi(\kappa_f-\kappa_s)}+R\Bigg]\frac{\theta''}{\nu_f}+\lambda_2\left(aF^2(\eta)\theta''(\eta)\right)+\frac{\mu_{nf}}{\left(\rho C_p\right)_{nf}}\frac{a^2x^2F''(\eta)^2}{\nu_f(T_w-T_\infty)}.$$

$$\Rightarrow -F(\eta)\theta'(\eta)=\frac{\kappa_f}{\phi(\rho C_p)_s+(1-\phi)(\rho C_p)_f}\Bigg[\frac{\kappa_s+2\kappa_f-2\phi(\kappa_f-\kappa_s)}{\kappa_s+2\kappa_f+\phi(\kappa_f-\kappa_s)}+R\Bigg]\frac{\theta''}{\nu_f}+\lambda_2\left(aF^2(\eta)\theta''(\eta)\right)+\frac{\mu_{nf}}{\phi(\rho C_p)_s+(1-\phi)(\rho C_p)_f}\frac{a^2x^2F''(\eta)^2}{\nu_f(T_w-T_\infty)}.$$

$$\Rightarrow -F(\eta)\theta'(\eta)=\frac{\kappa_f}{(\rho C_p)_f\left(1-\phi+\phi\frac{(\rho C_p)_s}{(\rho C_p)_f}\right)}\Bigg[\frac{\kappa_s+2\kappa_f-2\phi(\kappa_f-\kappa_s)}{\kappa_s+2\kappa_f+\phi(\kappa_f-\kappa_s)}+R\Bigg]\frac{\theta''}{\nu_f}+\lambda_2\left(aF^2(\eta)\theta''(\eta)\right)+\frac{\mu_{nf}}{(\rho C_p)_f\left(1-\phi+\phi\frac{(\rho C_p)_s}{(\rho C_p)_f}\right)}\frac{a^2x^2F''(\eta)^2}{\nu_f(T_w-T_\infty)}.$$

$$\Rightarrow -\left(1-\phi+\phi\frac{(\rho C_p)_s}{(\rho C_p)_f}\right)F(\eta)\theta'(\eta)=\frac{\kappa_f}{\nu_f(\rho C_P)_f}\Bigg[\frac{\kappa_s+2\kappa_f-2\phi(\kappa_f-\kappa_s)}{\kappa_s+2\kappa_f+\phi(\kappa_f-\kappa_s)}+R\Bigg]\frac{\theta''}{\nu_f}+\lambda_2aF^2(\eta)\theta''(\eta)\left(1-\phi+\phi\frac{(\rho C_p)_s}{(\rho C_p)_f}\right)+\frac{\mu_{nf}a^2x^2F''(\eta)^2}{(\rho C_p)_f\nu_f(T_w-T_\infty)}.$$

$$\Rightarrow -H_7F(\eta)\theta'(\eta) = \frac{1}{Pr}\left[\frac{\kappa_s + 2\kappa_f - 2\phi(\kappa_f - \kappa_s)}{\kappa_s + 2\kappa_f + \phi(\kappa_f - \kappa_s)} + R\right]\theta'' + \lambda_2 aF^2(\eta)\theta''(\eta)H_7 + \frac{\mu_{nf}a^2x^2F''(\eta)^2}{(\rho C_p)_f\nu_f(T_w - T_\infty)}.$$

Using (3.29) in above equation we get

$$-H_7F(\eta)\theta'(\eta) = H_6\theta''(\eta) + \lambda_2 aF^2(\eta)\theta''(\eta)H_7 + \frac{\mu_{nf}a^2x^2F''(\eta)^2}{(\rho C_p)_f\nu_f(T_w - T_\infty)},$$

$$\Rightarrow -H_7F(\eta)\theta'(\eta) = H_6\theta''(\eta) + \lambda_2 aF^2(\eta)\theta''(\eta)H_7 + \frac{\mu_f a^2x^2F''(\eta)^2}{(1-\phi)^{2.5}(\rho C_p)_f\nu_f(T_w - T_\infty)}.$$

$$\Rightarrow -H_7F(\eta)\theta'(\eta) = H_6\theta''(\eta) + \lambda_2 aF^2(\eta)\theta''(\eta)H_7 + \frac{H_1\mu_f a^2x^2F''(\eta)^2}{(\rho C_p)_f\nu_f(T_w - T_\infty)}.$$

$$\Rightarrow -H_7F(\eta)\theta'(\eta) = H_6\theta''(\eta) + \lambda_2 aF^2(\eta)\theta''(\eta)H_7 + \frac{H_1\mu_f a^2x^2F''(\eta)^2}{\rho_f(C_p)_f\nu_f(T_w - T_\infty)}.$$

$$\Rightarrow -H_7F(\eta)\theta'(\eta) = H_6\theta''(\eta) + \lambda_2 aF^2(\eta)\theta''(\eta)H_7 + \frac{\nu_f H_1 a^2x^2F''(\eta)^2}{(C_p)_f\nu_f(T_w - T_\infty)}.$$

$$\Rightarrow -H_7F(\eta)\theta'(\eta) = H_6\theta''(\eta) + \lambda_2 aF^2(\eta)\theta''(\eta)H_7 + \frac{H_1 a^2x^2F''(\eta)^2}{(C_p)_f(T_w - T_\infty)}.$$

By using (4.5) in above equation we get

$$-H_7F(\eta)\theta'(\eta) = H_6\theta''(\eta) + \lambda_2 aF^2(\eta)\theta''(\eta)H_7 + H_1E_cF''(\eta)^2,$$

$$\Rightarrow \quad -H_7F(\eta)\theta'(\eta) = H_6\theta''(\eta) + \gamma F^2(\eta)\theta''(\eta)H_7 + H_1E_cF''(\eta)^2.$$

$$\Rightarrow \quad H_6\theta''(\eta) + \gamma F^2(\eta)\theta''(\eta)H_7 + H_7F(\eta)\theta'(\eta) + H_1E_cF''(\eta)^2 = 0.$$

$$\Rightarrow H_6\theta''(\eta) + H_7\left(\gamma F^2(\eta)\theta''(\eta) + F(\eta)\theta'(\eta)\right) + H_1E_cF''(\eta)^2 = 0. \tag{4.8}$$

4.5 Solution Methodology

The shooting technique is used to solve the ordinary differential equation (4.8). The following notations have been considered:

$$\theta = L_1, \qquad \theta' = L_1' = L_2, \quad \theta'' = L_2'.$$

For simplification, the following notation have been defined.

$$H_6 = \frac{\left(\frac{\kappa_s+2\kappa_f-2\phi(\kappa_f-\kappa_s)}{\kappa_s+2\kappa_f+\phi(\kappa_f-\kappa_s)}+R\right)}{Pr}, \qquad H_7 = 1-\phi+\phi\frac{(\rho C_p)_s}{(\rho C_p)_f},$$
$$E_c = \frac{a^2x^2}{(C_p)_f(T_w-T_\infty)}.$$

By using the notations, the equation (4.8) is converted into first order ODEs.

$$L_1' = L_2, \qquad L_1(0) = 1,$$
$$L_2' = \frac{1}{H_6+H_7\gamma F^2(\eta)}[-H_7F(\eta)\theta'(\eta)+\frac{H_1}{H_7}E_cF''(\eta)], \qquad L_3(0) = s.$$

The above initial value problem will be numerically solved by RK-4. The missing condition s is to be chosen such that:

$$L_2(s) = 0.$$

To solve the above algebraic equation, we use the Newton's method which has the following iterative scheme:

$$s^{n+1} = s^n - \frac{(L_2(s))_{s=s^n}}{\left(\frac{\partial L_2(s)}{\partial s}\right)_{s=s^n}},$$

We further introduce the following notations, in order to obtain the derivative.

$$\frac{\partial L_1}{\partial s} = L_4, \qquad \frac{\partial L_2}{\partial s} = L_5, \qquad \frac{\partial L_3}{\partial s} = L_6.$$

As a result of these new notations, the Newton's iterative scheme, gets the form

$$s^{n+1} = s^n - \frac{(L_2(s)_{s=s^n}}{(L_5(s)_{s=s^n}}.$$

Now differentiate the last system of two first order ODEs with respect to s,

$$L_3' = L_4, \qquad L_3(0) = 0,$$
$$L_4' = \frac{1}{H_6+H_7\gamma F^2(\eta)}[-H_7F(\eta)L_4], \qquad L_4(0) = 1.$$

The stopping criteria for the Newton's method is set as:

$$| (L_2(s)_{s=s^n} | < \epsilon,$$

where ϵ is an arbitrarily small positive number. From now onward ϵ has been taken as 10^{-10}.

4.6 Analysis of Graphs and Tables

In this section, we have studied the Tiwari-Das model by adding viscous dissipation and Catteneo-Christov heat flux in energy equation to analyze the transfer of heat and flow through the boundary layer of a micro polar magnetite ferro fluid over a stretching and shrinking sheet under the effect of thermal radiation.The remaining two momentum equation are remain unchanged because we are only concerned with energy equation . The effects of parameters like suction and injection, radiation, magnetic, micro rotation, boundary parameters and Prandtl number on $F'(\eta)$, G(η) and $\theta(\eta)$ are observed for stretching and shrinking cases, separately. A thorough discussion on the graphs and tables has been conducted which contains the impact of dimensionless parameters on the local Nusselt number $(Re_x)^{\frac{-1}{2}} Nu_x$. Table 4.1 explains the impact of different parameter on the Nusselt number $(Re_x)^{\frac{-1}{2}} Nu_x$. For the rising values of ϕ, the Nusselt number decreases. It is evident that an increase in the micro rotation parameter ϕ, M, E_c and γ, the Nusselt number decreases while, it increases by increasing the values of K, M, S, α and δ. The missing conditions are taken within the interval represented by s, t and w.

Figures 4.1 shows the energy profile for suction and stretching for different values of R. The results show that if we increase the values of R, the energy profile increases. The dotted lines represent the energy field for micro polar nanofluid while the continuous lines represent the classical micropolar fluid.

Figure 4.2 shows the comparative analysis of micropolar fluid with some nano particles in it and fluid in pure form in case of injection and stretching for different

values of R. The energy profile increases as the value of R increases.

Figure 4.3 shows the velocity of micropolar fluid with some nano particles in it and fluid in pure form field. The graph and table shows that the temperature field increases in case of suction and stretching when we increase the value of R and in this case the value of micro rotation vector K is taken as zero.

Figure 4.4 represents the comparison of experimental data on micro polar fluid of Turkyilmazoglu [45] and temperature for different values of R in case of injection and stretching. The graph and table shows that the temperature field increases in case of injection and stretching when we increase the value of R and in this case the value of micro rotation vector K is taken as zero Figure 4.5 shows the contrast of velocity field and experimental data on micro polar fluid on micro polar fluid of Turkyilmazoglu [45]. The velocity profile increases with increase in values of K Figure 4.6 represents the contrast of temperature with experimental data on micro polar fluid for different values of K and graph shows that the energy profile increases with an increase in the values of K

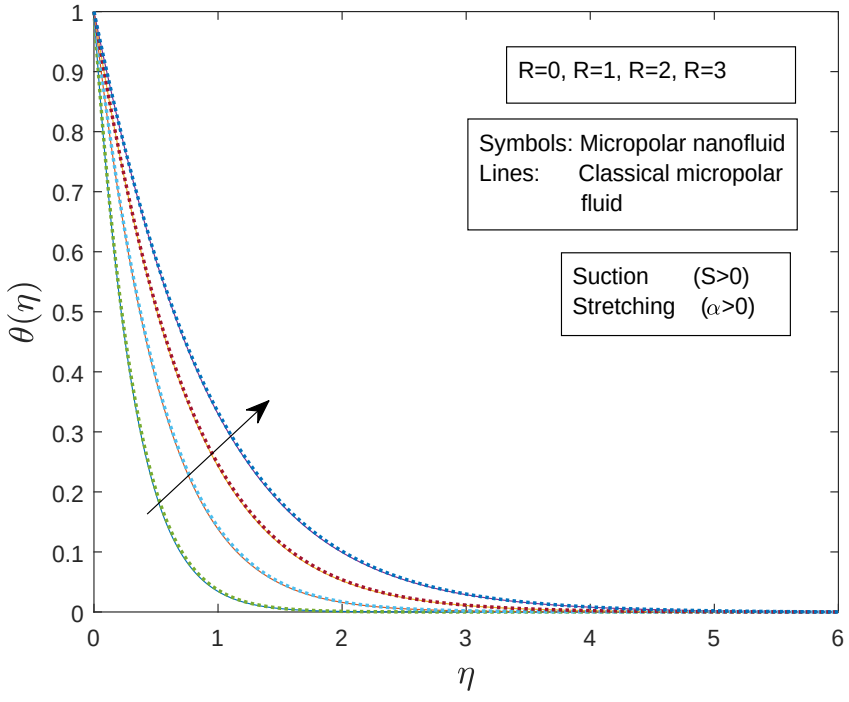

FIGURE 4.1: Impact of R on velocity profile for nanoparticles for suction and stretching .

TABLE 4.1: Results of $Re^{\frac{1}{2}}Cf_x$ for various parameters

ϕ	K	M	S	α	E_c	γ	$-(Re_x^{\frac{-1}{2}})Nu_x$	s	t	w
0.01	0.2	0.4	0.5	0.5	0.7	0.1	2.143472	[-0.5,10]	[-5,4]	[-10,10]
0.05							2.012606	[-0.5,10]	[-5,5]	[-10,10]
0.1							1.856045	[-0.5,10]	[-5,5]	[-10,10]
0.2							1.560458	[-0.5,5]	[-5,5]	[-10,10]
	0.1						2.142637	[-0.5,5]	[-5,5]	[-10,10]
	1						2.144424	[-0.5,5]	[-5,1]	[-10,10]
	1.5						2.142877	[-0.5,5]	[-5,1]	[-10,10]
	1.7						2.142099	[-0.5,5]	[-5,5]	[-10,10]
		1					2.138719	[-0.5,5]	[-5,5]	[-10,10]
		2					2.129011	[-0.5,5]	[-5,5]	[-10,10]
		3					2.119735	[-1,5]	[-5,5]	[-10,10]
		4					2.111355	[-1,5]	[-5,5]	[-10,10]
			0.1				1.109603	[-1,4]	[-5,5]	[-10,10]
			0.3				1.648827	[-1,5]	[-5,5]	[-10,10]
			1.0				2.934839	[-1,5]	[-5,5]	[-10,10]
			2.0				3.012396	[1,5]	[-5,5]	[-10,10]
				0.3			2.068160	[-0.5,5]	[-5,5]	[-10,10]
				0.6			2.166627	[-1,5]	[-5,5]	[-10,10]
				0.8			2.189994	[-1,5]	[-5,5]	[-10,10]
				0.9			2.191789	[-1,5]	[-5,5]	[-10,10]
					0.2		2.195003	[-0.5,5]	[-5,3]	[-10,10]
					0.9		2.122859	[-1,5]	[-5,5]	[-10,10]
					1		2.112553	[-0.5,5]	[-5,5]	[-10,10]
					1.5		2.061021	[-0.5,5]	[-5,3]	[-10,10]
						1	0.874236	[-0.5,5]	[-5,3]	[-10,10]
						1.5	0.657441	[-0.5,5]	[-5,5]	[-10,10]
						2	0.537587	[-0.5,5]	[-5,3]	[-10,10]
						2.5	0.463486	[-0.5,5]	[-5,3]	[-10,10]

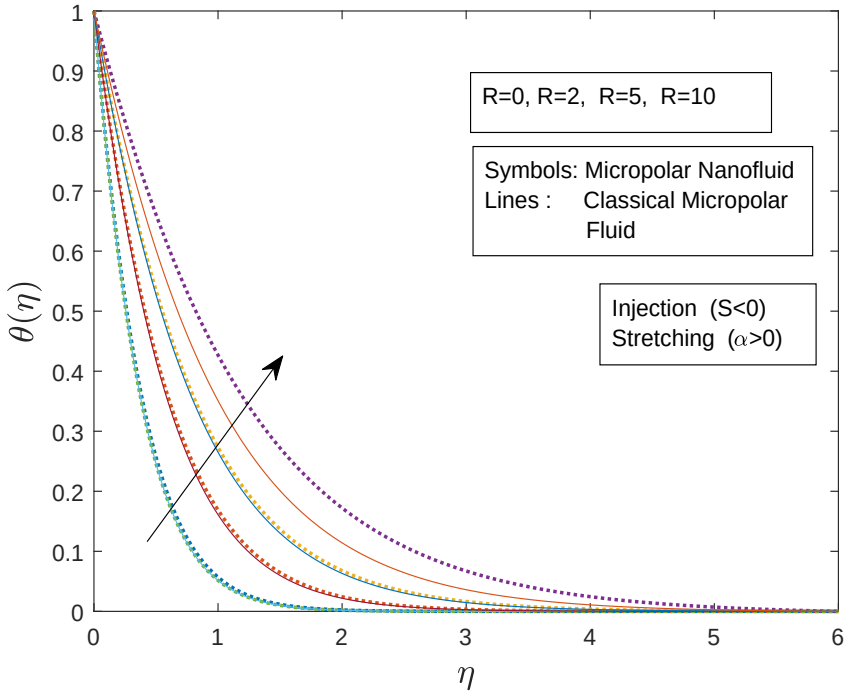

FIGURE 4.2: Impact of R on velocity profile for Injection and stretching .

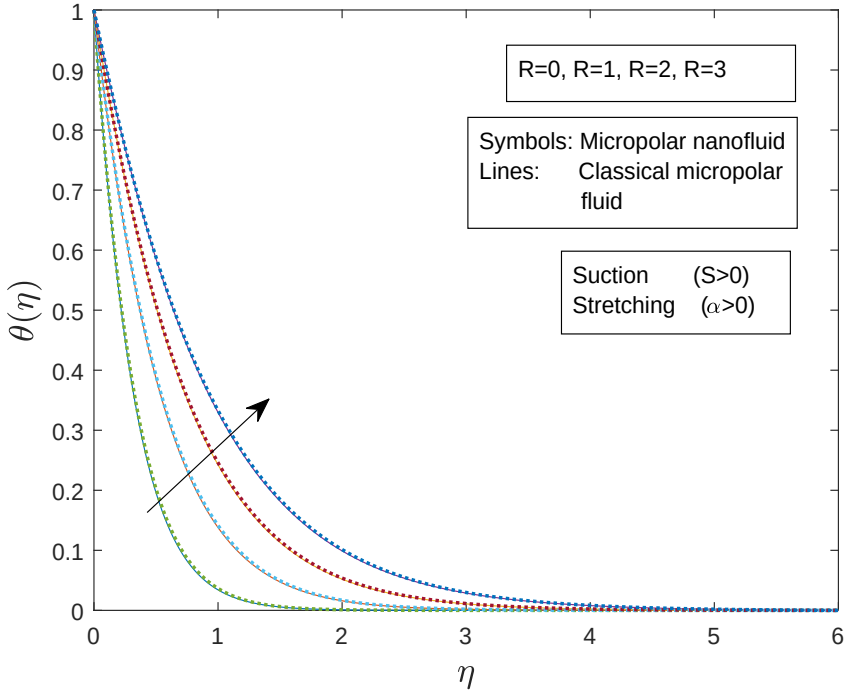

FIGURE 4.3: Impact of R on velocity profile for nanoparticles for suction and stretching at K=0.

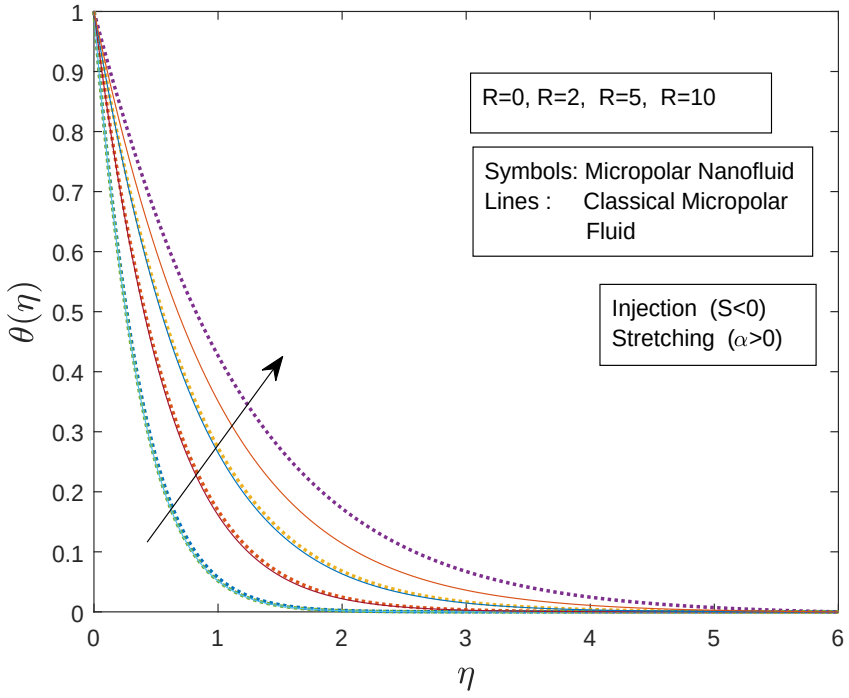

FIGURE 4.4: Impact of R on velocity profile for Injection and stretching at K=0.

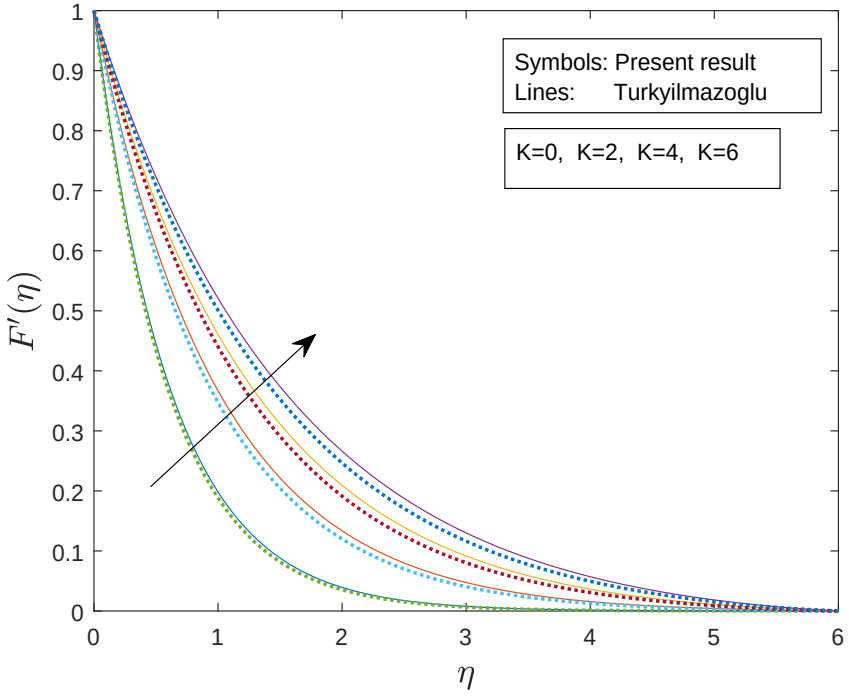

FIGURE 4.5: Impact of R on velocity profile for Injection and stretching .

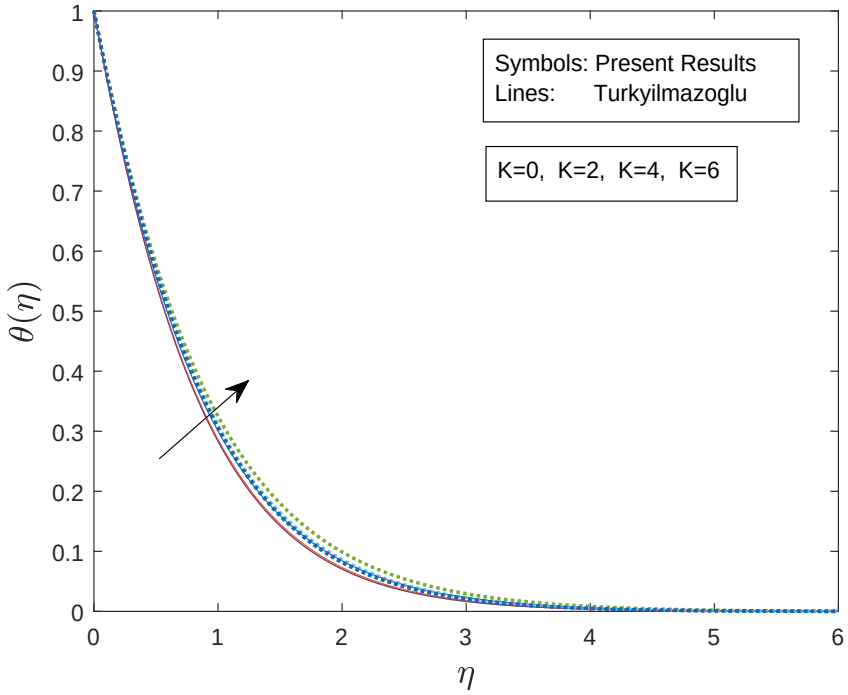

FIGURE 4.6: Impact of R on velocity profile for Injection and stretching .

Chapter 5

Conclusion

In this proposal, we have reviewed the work of Abid Hussanan, Mohd Zuki Salleh and Ilyas khan et al. [47] and extended with the effect of viscous dissipation and Cattaneo-Christov heat transition. Firstly, we convert the momentum and energy equation into ODEs by using similarity transformation. By using shooting technique, numerical solution can be find out for the transformed ODEs. By considering different governing physical parameters, the result are presented in the form of tables and graph for velocity and temperature profiles. The achievement of the current research can be summarized as below:

- Increasing the values of M, the velocity profile decreases for suction and stretching.
- Rising the values of M, the velocity profile decreases for injection and stretching.
- By enhancing the values of M, the velocity profile increases for suction and shrinking.
- Increasing the values of M, the velocity profile increases for injection and shrinking.
- The velocity profile increases for suction and stretching for the increasing value of K.

- Rising the values of K, the velocity profile increases for injection and stretching.
- Increasing the values of K, the velocity profile decreases for suction and shrinking.
- An increment is noticed in the velocity profile distribution by rising the value of K.
- Rising the values of δ, the velocity profile decreases for injection and stretching.
- With a rise in the values of R, the temperature profile increases for suction and stretching.
- Rising the values of R, the temperature profile increases for injection and stretching.
- Due to the ascending values of K, the temperature profile increases.

Bibliography

[1] S. U. Choi and J. A. Eastman, "Enhancing thermal conductivity of fluids with nanoparticles," 1995.

[2] R. Pal, "A novel method to determine the thermal conductivity of interfacial layers surrounding the nanoparticles of a nanofluid," *Nanomaterials*, vol. 4, no. 4, pp. 844–855, 2014.

[3] M. H. Bahmani, G. Sheikhzadeh, M. Zarringhalam, O. A. Akbari, A. A. Alrashed, G. A. S. Shabani, and M. Goodarzi, "Investigation of turbulent heat transfer and nanofluid flow in a double pipe heat exchanger," *Advanced Powder Technology*, vol. 29, no. 2, pp. 273–282, 2018.

[4] M. Bahiraei, M. Jamshidmofid, and M. Goodarzi, "Efficacy of a hybrid nanofluid in a new microchannel heat sink equipped with both secondary channels and ribs," *Journal of Molecular Liquids*, vol. 273, pp. 88–98, 2019.

[5] B. C. Pak and Y. I. Cho, "Hydrodynamic and Heat Transfer study of Dispersed Fluids with Submicron Metallic Oxide Particles," *Experimental Heat Transfer; an International Journal*, vol. 11, no. 2, pp. 151–170, 1998.

[6] J. Eastman, "Novel Thermal Properties of nanostructured Materials." 1999.

[7] Q. Li and Y. Xuan, "Convective Heat Transfer and Flow Characteristics of Cu-water nanofluid," *Science in China Series E: Technolgical Science*, vol. 45, no. 4, pp. 408–416, 2002.

[8] F. Rashidi and N. M. Nezamabad, "Experimental investigation of convective heat transfer coefficient of cnts nanofluid under constant heat flux," vol. 3, pp. 6–8, 2011.

[9] N. K. Mahanta and A. R. Abramson, "Thermal conductivity of graphene and graphene oxide nanoplatelets," pp. 1–6, 2012.

[10] B. Sun, W. Lei, and D. Yang, "Flow and convective heat transfer characteristics of fe2o3-water nanofluids inside copper tubes," *International Communications in Heat and Mass Transfer*, vol. 64, pp. 21–28, 2015.

[11] R. Walvekar, M. K. Siddiqui, S. Ong, and A. F. Ismail, "Application of cnt nanofluids in a turbulent flow heat exchanger," *Journal of Experimental Nanoscience*, vol. 11, no. 1, pp. 1–17, 2016.

[12] J. Buongiorno and L.-w. Hu, "Nanofluid heat transfer enhancement for nuclear reactor applications," vol. 43918, pp. 517–522, 2009.

[13] K. Das, "Slip effects on heat and mass transfer in mhd micropolar fluid flow over an inclined plate with thermal radiation and chemical reaction," *International journal for numerical methods in fluids*, vol. 70, no. 1, pp. 96–113, 2012.

[14] A. Kuznetsov and D. Nield, "Natural convective boundary-layer flow of a nanofluid past a vertical plate," *International Journal of Thermal Sciences*, vol. 49, no. 2, pp. 243–247, 2010.

[15] A. Noghrehabadi, R. Pourrajab, and M. Ghalambaz, "Flow and heat transfer of nanofluids over stretching sheet taking into account partial slip and thermal convective boundary conditions," *Heat and Mass Transfer*, vol. 49, no. 9, pp. 1357–1366, 2013.

[16] W. N. Mutuku and O. D. Makinde, "Hydromagnetic bioconvection of nanofluid over a permeable vertical plate due to gyrotactic microorganisms," *Computers & Fluids*, vol. 95, pp. 88–97, 2014.

[17] H. Xu and I. Pop, "Fully developed mixed convection flow in a horizontal channel filled by a nanofluid containing both nanoparticles and gyrotactic microorganisms," *European Journal of Mechanics-B/Fluids*, vol. 46, pp. 37–45, 2014.

[18] W. Khan and O. Makinde, "Mhd nanofluid bioconvection due to gyrotactic microorganisms over a convectively heat stretching sheet," *International Journal of Thermal Sciences*, vol. 81, pp. 118–124, 2014.

[19] K. Zaimi, A. Ishak, and I. Pop, "Boundary layer flow and heat transfer over a nonlinearly permeable stretching/shrinking sheet in a nanofluid," *Scientific Reports*, vol. 4, no. 1, pp. 1–8, 2014.

[20] W. A. Khan, J. R. Culham, and O. D. Makinde, "Combined heat and mass transfer of third-grade nanofluids over a convectively-heated stretching permeable surface," *The Canadian Journal of Chemical Engineering*, vol. 93, no. 10, pp. 1880–1888, 2015.

[21] M. Qasim, Z. Khan, R. Lopez, and W. Khan, "Heat and mass transfer in nanofluid thin film over an unsteady stretching sheet using buongiornos model," *The European Physical Journal Plus*, vol. 131, no. 1, pp. 1–11, 2016.

[22] N. S. Akbar, O. A. Bég, and Z. Khan, "Magneto-nanofluid flow with heat transfer past a stretching surface for the new heat flux model using numerical approach," *International Journal of Numerical Methods for Heat & Fluid Flow*, 2017.

[23] S. T. Mohyud-Din, U. Khan, N. Ahmed, and B. Bin-Mohsin, "Heat and mass transfer analysis for mhd flow of nanofluid inconvergent/divergent channels with stretchable walls using buongiornos model," *Neural Computing and Applications*, vol. 28, no. 12, pp. 4079–4092, 2017.

[24] U. Khan, N. Ahmed, S. T. Mohyud-Din, and B. Bin-Mohsin, "Nonlinear radiation effects on mhd flow of nanofluid over a nonlinearly stretching/shrinking wedge," *Neural Computing and Applications*, vol. 28, no. 8, pp. 2041–2050, 2017.

[25] M. Sheikholeslami and H. B. Rokni, "Effect of melting heat transfer on nanofluid flow in existence of magnetic field considering buongiorno model," *Chinese Journal of Physics*, vol. 55, no. 4, pp. 1115–1126, 2017.

[26] M. Sheikholeslami, D. Ganji, and M. Rashidi, "Magnetic field effect on unsteady nanofluid flow and heat transfer using buongiorno model," *Journal of Magnetism and Magnetic Materials*, vol. 416, pp. 164–173, 2016.

[27] M. A. Sheremet and I. Pop, "Free convection in a porous horizontal cylindrical annulus with a nanofluid using buongiornos model," *Computers & Fluids*, vol. 118, pp. 182–190, 2015.

[28] A. J. Ahrar and M. H. Djavareshkian, "Computational investigation of heat transfer and entropy generation rates of al2o3 nanofluid with buongiorno's model and using a novel tvd hybrid lb method," *Journal of Molecular Liquids*, vol. 242, pp. 24–39, 2017.

[29] M. Mustafa, "Mhd nanofluid flow over a rotating disk with partial slip effects: Buongiorno model," *International Journal of Heat and Mass Transfer*, vol. 108, pp. 1910–1916, 2017.

[30] R. Ahmad, M. Mustafa, and S. Hina, "Buongiorno's model for fluid flow around a moving thin needle in a flowing nanofluid: A numerical study," *Chinese Journal of Physics*, vol. 55, no. 4, pp. 1264–1274, 2017.

[31] W. Yu, D. M. France, D. Singh, E. V. Timofeeva, D. S. Smith, and J. L. Routbort, "Mechanisms and models of effective thermal conductivities of nanofluids," *Journal of Nanoscience and Nanotechnology*, vol. 10, no. 8, pp. 4824–4849, 2010.

[32] N. A. Yacob, A. Ishak, I. Pop, and K. Vajravelu, "Boundary layer flow past a stretching/shrinking surface beneath an external uniform shear flow with a convective surface boundary condition in a nanofluid," *Nanoscale Research Letters*, vol. 6, no. 1, pp. 1–7, 2011.

[33] K. Vajravelu, K. Prasad, J. Lee, C. Lee, I. Pop, and R. A. Van Gorder, "Convective heat transfer in the flow of viscous ag–water and cu–water nanofluids over a stretching surface," *International Journal of Thermal Sciences*, vol. 50, no. 5, pp. 843–851, 2011.

[34] M. Hamad, "Analytical solution of natural convection flow of a nanofluid over a linearly stretching sheet in the presence of magnetic field," *International communications in heat and mass transfer*, vol. 38, no. 4, pp. 487–492, 2011.

[35] M. Hamad, I. Pop, and A. M. Ismail, "Magnetic field effects on free convection flow of a nanofluid past a vertical semi-infinite flat plate," *Nonlinear Analysis: Real World Applications*, vol. 12, no. 3, pp. 1338–1346, 2011.

[36] M. Sheikholeslami, M. Hatami, and D. Ganji, "Analytical investigation of mhd nanofluid flow in a semi-porous channel," *Powder Technology*, vol. 246, pp. 327–336, 2013.

[37] M. Sheikholeslami and D. Ganji, "Heat transfer of cu-water nanofluid flow between parallel plates," *Powder Technology*, vol. 235, pp. 873–879, 2013.

[38] A. Ebaid and M. A. Al Sharif, "Application of laplace transform for the exact effect of a magnetic field on heat transfer of carbon nanotubes-suspended nanofluids," *Zeitschrift für Naturforschung A*, vol. 70, no. 6, pp. 471–475, 2015.

[39] R. Kandasamy, R. Mohamad, and M. Ismoen, "Impact of chemical reaction on cu, al2o3 and swcnts–nanofluid flow under slip conditions," *Engineering Science and Technology, an International Journal*, vol. 19, no. 2, pp. 700–709, 2016.

[40] A. Hussanan, I. Khan, H. Hashim, M. K. Anuar, N. Ishak, N. M. Sarif, and M. Z. Salleh, "Unsteady mhd flow of some nanofluids past an accelerated vertical plate embedded in a porous medium," *Jurnal Teknologi*, vol. 78, no. 2, 2016.

[41] H. Saleh, E. Alali, and A. Ebaid, "Medical applications for the flow of carbon-nanotubes suspended nanofluids in the presence of convective condition using laplace transform," *Journal of the association of Arab universities for basic and applied sciences*, vol. 24, pp. 206–212, 2017.

[42] A. C. Eringen, "Theory of micropolar fluids," *Journal of Mathematics and Mechanics*, pp. 1–18, 1966.

[43] I. Hassanien and R. Gorla, "Heat transfer to a micropolar fluid from a non-isothermal stretching sheet with suction and blowing," *Acta Mechanica*, vol. 84, no. 1, pp. 191–199, 1990.

[44] A. Mohammadein and R. S. R. Gorla, "Heat transfer in a micropolar fluid over a stretching sheet with viscous dissipation and internal heat generation," *International Journal of Numerical Methods for Heat & Fluid Flow*, 2001.

[45] M. Turkyilmazoglu, "Flow of a micropolar fluid due to a porous stretching sheet and heat transfer," *International Journal of Non-Linear Mechanics*, vol. 83, pp. 59–64, 2016.

[46] A. Hussanan, M. Z. Salleh, I. Khan, and R. M. Tahar, "Heat and mass transfer in a micropolar fluid with newtonian heating: an exact analysis," *Neural Computing and Applications*, vol. 29, no. 6, pp. 59–67, 2018.

[47] A. Hussanan, M. Z. Salleh, and I. Khan, "Microstructure and inertial characteristics of a magnetite ferrofluid over a stretching/shrinking sheet using effective thermal conductivity model," *Journal of Molecular Liquids*, vol. 255, pp. 64–75, 2018.

[48] H. Waqas, S. Hussain, H. Sharif, and S. Khalid, "Mhd forced convective flow of micropolar fluids past a moving boundary surface with prescribed heat flux and radiation," *Journal of Advances in Mathematics and Computer Science*, pp. 1–14, 2017.

[49] S. H. M. Saleh, N. M. Arifin, R. Nazar, and I. Pop, "Unsteady micropolar fluid over a permeable curved stretching shrinking surface," *Mathematical Problems in Engineering*, vol. 2017, 2017.

[50] K.-L. Hsiao, "Micropolar nanofluid flow with mhd and viscous dissipation effects towards a stretching sheet with multimedia feature," *International Journal of Heat and Mass Transfer*, vol. 112, pp. 983–990, 2017.

[51] P. J. Pritchard, R. W. Fox, and A. T. McDonald, *Introduction to fluid mechanics*. John Wiley & Sons, 2010.

[52] R. Bansal, *A Textbook of Fluid Mechanics*. Firewall Media, 2005.

[53] J. N. Reddy and D. K. Gartling, *The Finite Element Method in Heat Transfer and Fluid Dynamics*. CRC press, 2010.

[54] J. Ahmed and M. S. Rahman, *Handbook of Food Process Design, 2 Volume Set*. John Wiley & Sons, 2012.

[55] J. Koo and C. Kleinstreuer, "Viscous dissipation effects in microtubes and microchannels," *International journal of heat and mass transfer*, vol. 47, no. 14-16, pp. 3159–3169, 2004.

[56] X. Li, A. U. Khan, M. R. Khan, S. Nadeem, and S. U. Khan, "Oblique stagnation point flow of nanofluids over stretching/shrinking sheet with cattaneo–christov heat flux model: existence of dual solution," *Symmetry*, vol. 11, no. 9, p. 1070, 2019.

[57] A. Soward, "An introduction to magnetohydrodynamics. by pa davidson. cambridge university press, 2001. 431 pp. isbn 0 521 79149 9.£ 70.00 (hardback); isbn 0 521 79487 0.£ 24.95 (paperback)." *Journal of Fluid Mechanics*, vol. 450, pp. 408–410, 2002.

[58] R. W. Lewis, P. Nithiarasu, and K. N. Seetharamu, *Fundamentals of the finite element method for heat and fluid flow*. John Wiley & Sons, 2004.

[59] M. Gad-el Hak, *Frontiers in experimental fluid mechanics*. Springer Science & Business Media, 2013, vol. 46.

[60] T.Y.Na, *Computational methods in engineering boundary value problems.* Academic press, 1979.